International Journal of
Molecular Sciences

MDPI

Review

Mineral Carbonation for Carbon Sequestration: A Case for MCP and MICP

Samantha M. Wilcox [1], Catherine N. Mulligan [1,*] and Carmen Mihaela Neculita [2]

[1] Department of Building, Civil and Environmental Engineering, Concordia University, Montréal, QC H3G IM8, Canada; wilcox.samantha@gmail.com
[2] Research Institute on Mines and the Environment (RIME), University of Quebec in Abitibi-Témiscamingue, Rouyn-Noranda, QC J9X 5E4, Canada; carmenmihaela.neculita@uqat.ca
* Correspondence: mulligan@civil.concordia.ca

Abstract: Mineral carbonation is a prominent method for carbon sequestration. Atmospheric carbon dioxide (CO_2) is trapped as mineral carbonate precipitates, which are geochemically, geologically, and thermodynamically stable. Carbonate rocks can originate from biogenic or abiogenic origin, whereby the former refers to the breakdown of biofragments and the latter precipitation out of water. Carbonates can also be formed through biologically controlled mechanisms (BCMs), biologically mediated mechanisms (BMMs), and biologically induced mechanisms (BIMs). Microbial carbonate precipitation (MCP) is a BMM occurring through the interaction of organics (extracellular polymeric substances (EPS), cell wall, etc.) and soluble cations facilitating indirect precipitation of carbonate minerals. Microbially induced carbonate precipitation (MICP) is a BIM occurring via different metabolic pathways. Enzyme-driven pathways (carbonic anhydrase (CA) and/or urease), specifically, are promising for the high conversion to calcium carbonate ($CaCO_3$) precipitation, trapping large quantities of gaseous CO_2. These carbonate precipitates can trap CO_2 via mineral trapping, solubility trapping, and formation trapping and aid in CO_2 leakage reduction in geologic carbon sequestration. Additional experimental research is required to assess the feasibility of MICP for carbon sequestration at large scale for long-term stability of precipitates. Laboratory-scale evaluation can provide preliminary data on preferable metabolic pathways for different materials and their capacity for carbonate precipitation via atmospheric CO_2 versus injected CO_2.

Keywords: mineral carbonation; carbon sequestration; carbon dioxide; microbially induced carbonate precipitation; urease; carbonic anhydrase; microbial carbonate precipitation

check for updates

Academic Editor: Jian Zhao

Received: 31 January 2025
Revised: 24 February 2025
Accepted: 27 February 2025
Published: 1 March 2025

Citation: Wilcox, S.M.; Mulligan, C.N.; Neculita, C.M. Mineral Carbonation for Carbon Sequestration: A Case for MCP and MICP. *Int. J. Mol. Sci.* **2025**, *26*, 2230. https://doi.org/10.3390/ijms26052230

1. Introduction

Global warming and climate change have been significant concerns to scientists, engineers, and policy makers for a long time. The first Intergovernmental Panel on Climate Change (IPCC) was held in 1988 and the notorious Paris Agreement in 2015, which involved a commitment by 195 countries to limit global warming to 1.5–2 °C. Today, despite efforts to reduce greenhouse gas (GHG) emissions, global warming is projected at 3.5 °C by 2100 [1]. There is a need for carbon sequestration strategies that transform and sequester GHGs (CO_2, methane (CH_4) and fluorinated gases (hydrofluorocarbons (HFCs), perfluorinated compounds (PFCs), sulfur hexafluoride (SF_6), and nitrogen trifluoride (NF_3)) from the atmosphere, which, left untreated, create a warming effect.

Biological carbon sequestration can utilize plants and microorganisms (bacteria, fungi, archaea, cyanobacteria, and algae) to fix inorganic CO_2 as organic products (cellulous, lignocellulose, chitin, hemicellulose, lignin, etc.) or mineral precipitates for carbon capture and utilization [2]. Some microorganisms (carboxydotrophs) are carbon dependent and utilize atmospheric CO and CO_2 as their energy source [3]. Further, there are many identified pathways and enzymes (e.g., CA, RuBisCO, carbon monoxide dehydrogenase (CODH), etc.) linked to biologic carbon sequestration [2]. Mineral carbonation, specifically, biogenic mineral carbonation, offers a promising opportunity to sequester atmospheric CO_2 through naturally occurring processes. The process can be applied passively (trapping atmospheric CO_2) or as a carbon capture and storage (CCS; actively injecting CO_2) strategy.

While microbially induced carbonate precipitation (MICP) is a well-studied biological technique for soil and cement strengthening and restoration of construction materials, limited research has evaluated its feasibility as a carbon sequestration technique. In short, the microorganisms act as a catalyst to chemical precipitation and capture carbon as mineral carbonate precipitates. These reactions can be naturally occurring or engineered to enhance or optimize precipitation and therefore carbon sequestration. Alternatively, microbial carbonate precipitation (MCP) is a passive precipitation technique driven by the organic material in the environment. The objective of this paper is to evaluate abiotic and biotic carbonation, making a case for MICP and MCP as viable mineral carbonation techniques for carbon sequestration.

2. Biochemical Precipitation

2.1. Carbonate Precipitates

Chemical precipitation is a complex process used for separation of solid substances from solution [4–6]. For precipitation to occur, the solute concentration must exceed the liquid–solid equilibrium of the solution, meaning it is in a supersaturated state [5]. Supersaturation is, therefore, the driving force of precipitation [4,5]. Thermodynamically, the Gibbs free energy (G) and the solubility product constant (K_{sp}) govern the reaction equilibria and the solubility equilibria, respectively [7].

Kinetically, there are three main processes that direct precipitation. These include nucleation, growth, and agglomeration [5]. Nucleation refers to the birth of particles via condensation of ions. It can be homogenous (spontaneous) or heterogenous (prompted by foreign particles) [5,7]. Growth and agglomeration refer to the enlargement of particles. Crystal growth refers to the enlargement from material deposition onto formed particles via transport to the crystal surface, adsorption onto the crystal surface, or formation of crystal lattice bonds [7]. Agglomeration refers to the contact of two or more particles, which over time forms a stable particle [5]. The supersaturation will impact the type of nucleation and growth, which affects the texture and purity of the crystals [5]. Precipitates can also undergo aging (re-arrangement of the crystal structure to form larger, pure crystals with time) and coprecipitation (ion inclusion into the crystal structure or adsorption onto the crystal surface) [7]. Chemical precipitation factors include the soil–water system, pH (favors high pH), Eh, type and concentration of metals and metalloids (metal(loid)s), dissolved organic carbon (DOC), and inorganic and organic ligand presence [8].

Carbonate rocks can exist as igneous [9], sedimentary [10], and metamorphic rocks [11]. However, they primarily present as sedimentary rocks, either as limestone ($CaCO_3$; calcite and aragonite) or dolostone ($CaMg(CO_3)_2$) [12]. However, minerals are distinct from rocks, and there are numerous carbonate minerals: magnesite ($MgCO_3$), siderite ($FeCO_3$), dolomite ($CaMg(CO_3)_2$), otavite ($CdCO_3$), rhodochrosite ($MnCO_3$), cerussite ($PbCO_3$), smithsonite ($ZnCO_3$), strontianite ($SrCO_3$), witherite ($BaCO_3$), etc. Calcium carbonate is the most abundant of the carbonate minerals, occurring as calcite, aragonite, and vaterite anhydrous polymorphs [10,12], whereby calcite is the most thermodynamically stable and vaterite is the least. Less reported are the hydrous (monoclinic ikaite ($CaCO_3 \cdot 6H_2O$)

and calcium carbonate monohydrate ($CaCO_3 \cdot H_2O$)) and amorphous (ACC–$CaCO_3 \cdot nH_2O$) polymorphs [12].

The crystal structure and morphology of carbonate minerals varies significantly. Calcite and dolomite typically have a hexagonal crystallography, whereas aragonite is usually an orthorhombic structure [13,14]. However, the degree of supersaturation has been shown to alter the crystal form [15]. This is in conjunction with morphologic changes in the minerals due to crystal growth rate dependent on supersaturation [12,16]. Therefore, the solubility of carbonate minerals is essential to crystal formation. The reversible reaction for $CaCO_3$ dissolution and precipitation is shown in Equation (1), where the rightward reaction illustrates the dissolution of carbonate minerals, and the leftward reaction demonstrates precipitation [12]. Relative solubility is impacted by crystal size, heterogeneity, defects, porosity, and organic matrices, with mineralogy the most significant [12]. Magnesium (Mg^{2+}), for example, is known to inhibit calcite growth [16–18] and increase calcite solubility [12]. Furthermore, CO_2 concentration impacts solubility and precipitation, in which an increase in CO_2 also increases $CaCO_3$ solubility, causing dissolution [12,19]. Temperature and pressure also influence calcite formation, since temperature and pressure increases can cause $CaCO_3$ solubility decreases, which favors precipitation [12,19,20]. It should be noted that CO_2 solubility is inversely correlated to temperature, and positively correlated to pressure [21].

$$CaCO_3 + H_2O + CO_2 \leftrightarrow Ca^{2+} + 2HCO_3^- \quad (1)$$

Carbonate minerals form carbonate rocks through deposition and diagenesis [12]. They are formed in marine (ocean, sea (neritic and pelagic)) and terrestrial (lakes, hot and cold springs, caves, soils) environments, originating from biogenic, abiogenic, or complex mixtures of both components [12]. Carbonate sediments can be categorized as deep-sea oozes, carbonate turbidites, shelf accumulations of lime sands, silts, muds, organic reefs, and reef debris [22]. They are classified according to their compositions, fabric, and origin [23]. The biosphere and depositional environment impact the skeleton mineralogic, petrographic, and geochemical vestiges of the carbonate rocks [12]. Biogenic deposition often refers to the breakdown of invertebrate biofragments (i.e., shells, single cells, colonial skeletons) and crystallites within algal tissue or the calcification of microbes (i.e., calcimicrobes), whereas abiogenic deposition results from precipitation out of seawater or freshwater [12]. Diagenesis is a complex process encompassing 30 processes, including lithification destructive processes, re-crystallization, and grain-diminution [24]. In Precambrian times, carbonate rocks originated from algae pH control in lagoons and direct chemical precipitation out of sea water, while Cambrian origin often resulted from the organisms extracting carbonate out of sea water [25].

2.2. Biogenic Carbonate Precipitates

Bioprecipitation can encompass the formation of all biologically facilitated crystalline or amorphous precipitates with both organic and/or inorganic components. Bioprecipitation uses microorganisms to catalyze chemical precipitation reactions. It can incorporate different microorganisms to facilitate distinct metabolic pathways. The aim is to precipitate compounds (i.e., carbonates, hydroxides, phosphates, sulfides, sulfates, arsenates, silicas, chlorides, fluorides, oxides, oxalates, etc. [26–29]) with low solubility.

Abiotic precipitation varies significantly from biotic precipitation. The morphology is a key indicator used to distinguish inorganic and abiotic processes from biogenic minerals [30], which are typically differentiated by their unusual external morphology [29]. An interesting characteristic of biominerals is the composites or agglomeration of crystals separated by organic material [29]. Researchers have found differences in shape, size, crystallinity, isotopic, trace compositions, organic functional groups, activation energy, and enthalpy between biotic and abiotic precipitates [29,30]. Within lacustrine systems, for example, carbonate minerals are typically of biological origin or from direct biological activity, whereby the oxic (bio-induced pelagic CO_3^{2-} precipitates), suboxic, and anoxic (microbial-induced diagenetic CO_3^{2-} precipitates) conditions in the microenvironment with the ion supply impact the microbial pathway (see Section 2.4) [31]. Therefore, microenvironmental conditions impact the carbon isotopic composition of dissolved inorganic carbon (DIC) in pore water and the carbon isotopic composition of precipitates [31]. Further differences have been reported between biotic, organogenic (nutrient composition without bacterial cells), and inorganogenic (chemical reaction) forms of $CaCO_3$ precipitation, suggesting thermal stability is highest in biotic calcite [30]. The calcite crystal growth rate and biotic growth rate in carbonate deposits will influence whether it is biotic/abiotic [32]. If the supersaturation state is high, calcite will favor abiotic precipitation, as crystal formation outpaces microbial growth rates [32]. In the context of carbon sequestration, abiotic factors regulating sequestration include pH and medium components (i.e., urea), while biotic factors are dependent on the species or strains [33]. Again, resident biota will impact the CO_2 levels inducing dissolution (water absorption of CO_2 respiration in soil increasing acidity and dissolution) or precipitation (removal of CO_2 in seawater via phototrophs during photosynthesis) [12]. The degree of control exerted by the microorganism will dictate the biological mechanism occurring [29].

The interaction between microbial activity, the external environmental conditions, and the overall biofilm matrix will determine how and whether biotic precipitates form. There are three primary mechanisms (Figure 1 and Table 1) capable of facilitating bioprecipitation, including biologically controlled mechanisms (BCMs), biologically induced mechanisms (BIMs), and biologically mediated mechanisms (BMMs; otherwise termed biologically influenced mechanisms). Under certain conditions, microorganisms can synthesize minerals via nucleation and growth facilitating BCM [26,27,29,34,35]. Cellular activities including active pumping, passive diffusion, and secretion can lead to precipitation of particles in the extracellular, intracellular, or intercellular environment [26,27,29]. The final resting place of precipitates is within or on the microbial cell [27,34,36]. The composition, morphology, and localization of precipitates are influenced by the species-specific process [26,29]. BIMs involve the metabolic activity of the microorganism, which interact with the environment to facilitate precipitation [26,27,29,36]. The precipitates form in the extracellular environment, where nucleation and growth typically transpire on the microbial cell wall [29]. Precipitation is dependent on the environmental conditions (i.e., pH, redox potential, CO_2, etc.) and the subsequent supersaturation [29,34,35,37]. The composition, particle size, crystal purity, and morphology are varied due to diverse environmental conditions [26,29]. Passive precipitation is caused by the BMM due to the interaction of organic matter (i.e., extracellular polymeric substances (EPS), biofilm, and the organic/inorganic compounds) within the matrix [26,34]. Biological activity does not directly cause precipitation.

Both BIM and BMM utilize prokaryotes to facilitate precipitation. While the presence of microorganisms is not directly required for BMM, the organic EPS matrix is an extension of the microbial cell [38], as shown in Figure 1. Mineral deposits via BIM and BMM can be classified as stromatolites, thrombolites, and leiolite [38]. For carbonate precipitation, the BIM and BMM are referred to as MICP and MCP, respectively. Table 2 provides a comparative analysis of these methods. For global carbon sequestration, MCP is well established as a long-term storage technique for carbon. Carbon can be trapped in terrestrial environments (i.e., soils, caves, deserts, tundra, boreal forests, temperate forests, tropical forests, grasslands, etc.) in the organic matrix of soil as soil organic carbon (SOC), carbonate deposits (precipitated via plants, fungi, or bacteria), and/or vegetation [38–40]. Plants are also able to store inorganic CO_2 through biological carbon mitigation as organic carbon through photosynthesis [41]. As a byproduct of photosynthesis, plants can precipitate whewellite ($Ca(C_2O_4)\cdot H_2O$) storing atmospheric CO_2 [38]. Liu et al. [42] found that EPS and EPS-carbon are positively correlated to SOC, whereby EPS-carbon accounts for $\leq$10.69% the total organic carbon in surface sediments. This is quite significant, since 75% of organic carbon is sequestered in mangrove ecosystems in sediments [42,43]. MICP, however, is less established in terms of global carbon sequestration. MICP is shown to store carbon as carbonate deposits in marine environments, hypersaline lakes, freshwater environments, and continental environments [38], which act as carbon sinks for carbon sequestration.

Table 1. Comparative analysis of BCM, BIM, and BMM. Adapted from [38,44].

Mechanism	Precipitate Location	Conditions	Organisms	Level of Organism Control	Precipitated Minerals
BCM	Intracellular, intercellular, extracellular	Controlled by cellular activities	Eukaryotes	High	Magnetite, greigite, amorphous silica, calcite
BIM	Extracellular	Reactive surfaces & metabolism	Prokaryotes	Moderate	Iron hydroxides, magnetite, manganese oxides, clays, amorphous silica, carbonates, phosphates, sulfates, sulfide minerals
BMM	EPS matrix	Alkalinity engine & organic matter	Not required	Low	Carbonate minerals

Table 2. Comparative analysis of MICP and MCP.

Carbonate Precipitation	Mechanism	Microbial Involvement	Application	Research Topics	Advantages	Drawbacks
MICP	BIM	Active	In situ [1] & ex situ [2]	Restoration of calcareous stones & construction materials, soil strengthening, selective plugging for oil recovery, bio-clogging, soil thermal conductivity, dust suppression, erosion control, liquefaction mitigation, wastewater treatment, bioremediation, CO_2 sequestration [45]	Wide range of applicable microorganisms, applicable to a wide range of environments, low costs, high $CaCO_3$ conversion, short timeframes [45]	Potential for harmful byproducts, bio-clogging at injection site, requires specific conditions
MCP	BMM	Passive	In situ [1] & ex situ [2]	Wastewater treatment, oil recovery, biofilm barriers, bioremediation [46]	Wide range of environments, adaptable to versatile environmental conditions	Variable efficacy for carbonate precipitation, slower rates of precipitation

[1] In situ biostimulation, ex situ biostimulation and bioaugmentation [47]. [2] Material pre-treatment [35].

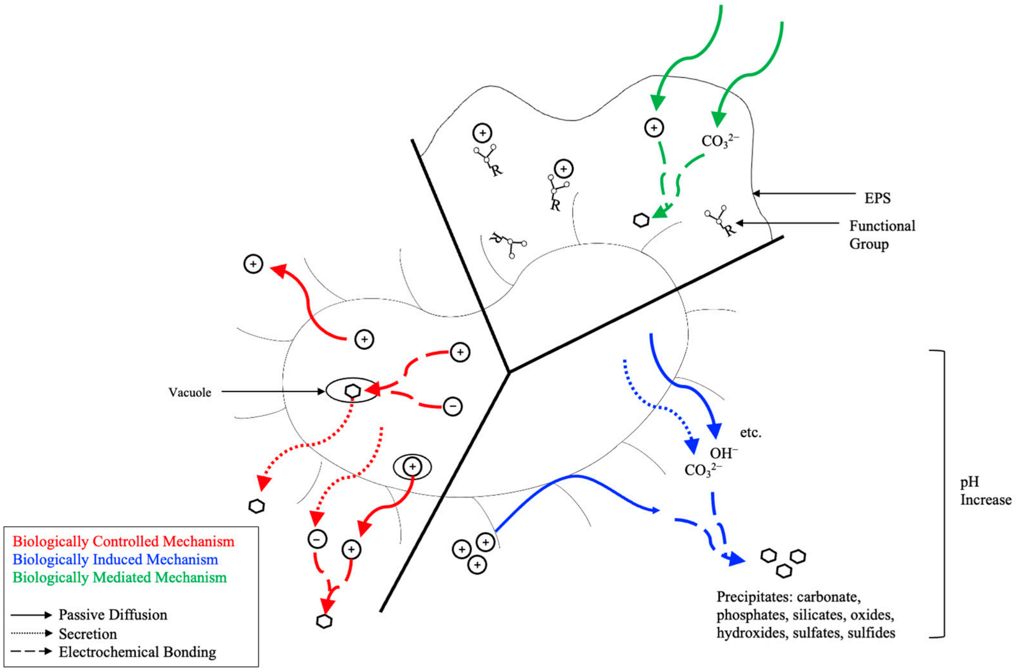

Figure 1. Biochemical precipitation mechanisms, including biologically controlled mechanisms (**left**), biologically induced mechanisms (**right**), and biologically mediated mechanisms (**top**). The red lines represent passive diffusion, blue lines represent active pumping, and green lines represent secretion. Adapted from [33,36,45].

It should be noted that in addition to bacterial carbonate precipitation, eukaryotes (i.e., *coccolithophores* and *foraminifera*) can precipitate carbonates to form shells or skeletons via BCM [44,48]. The formation of $CaCO_3$ exoskeletons plays an important role in the carbon cycle, impacting CO_2 flux in seawater and inorganic carbon transport in oceans and sediments [48]. *Coccolithophores*, specifically, are promising for global climate change because (i) they are phytoplankton (autotrophic plankton obtaining energy through photosynthesis); (ii) they produce dimethyl sulfide (DMS), creating albedo effects via formation of highly reflective clouds; (iii) they control CO_2 influx into water via precipitation of $CaCO_3$, which depletes dissolved bicarbonate (HCO_3^-), increasing dissolved CO_2 [44,48,49]. However, increased CO_2 has been shown to decrease $CaCO_3$ precipitation in marine phytoplankton [50], since increased atmospheric CO_2 also increases carbonic acid (H_2CO_3), producing more HCO_3^- and H^+ ions (Equation (2)), which dissolves $CaCO_3$, decreasing pH [48]. Furthermore, there are numerous autotropic carbon-fixation mechanisms identified in archaea, including the Calvin cycle, reductive citric acid cycle, reductive acetyl-coenzyme A pathway, 3-hydroxypropionate bicycle, hydroxypropionate-hydroxybutyrate cycle, and dicarboxylate-hydroxybutyrate cycle [51].

$$CO_2 + H_2O \leftrightarrow H_2CO_3 \leftrightarrow HCO_3^- + H^+ \leftrightarrow CO_3^{2-} + 2H^+ \tag{2}$$

2.3. Microbial Carbonate Precipitation (MCP)

The precipitation of $CaCO_3$ is dependent on the calcium (Ca^{2+}) concentration, DIC, nucleation sites, and pH [27,52]. For the purpose of microbial precipitation, the principal role of bacteria is to create an alkaline environment via pH and DIC increase [52]. This can occur as a BMM (passive process) or BIM (active process) [26].

Biologically mediated $CaCO_3$ precipitation occurs from the interaction of EPS and Ca^{2+} ions. As mentioned previously, the process does not require direct biological activity but is influenced by the organics associated with the cell wall and/or the EPS [26,34,37,53]. The microorganisms secrete natural polymers (polysaccharides, lipids, proteins, etc.), forming an organic matrix. These organic polymers favor heterogenous nucleation, leading to stabilization of new particles [37]. They can also act as nucleation sites [53,54]. Further, an increase in pH causes functional groups to deprotonate, causing exopolysaccharides produced by the microbial cell to have an overall negative charge and bind to metal(loid) ions [26].

The bacterial cell surface and biomass surfaces have an electronegative charge due to the presence of carboxyl, phosphoryl, amino, and sulfo groups [55]. The negative surface charge allows redox processes, adsorption, complexation, ion exchange, electrostatic attraction, and precipitation to immobilize metal(loid)s in situ [27,56]. For example, adsorption of positive divalent cations to the bacterial cell wall can lead to the precipitation of carbonates [27]. Initial adsorption of bacteria onto mineral surfaces is governed by hydrophobicity and electrostatic forces, while final attachment of bacteria to minerals is influenced by biofilm formation and secretion of exudates [57]. Therefore, uptake of cationic metal(loid)s can create a state of oversaturation in the microenvironment, leading to precipitation [58]. Further, both the cell wall and EPS have metal binding capacities; however, fate transport of these bonded metals is not known [59]. The bacterial cell wall provides nucleation sites for mineral deposition of biological precipitates [60,61]. This is in addition to exopolymers, biofilms, and inactive spores, which also provide sites for nucleation [26].

The function of EPS is important to the carbonate precipitation process. EPS are high-molecular-weight natural polymers (i.e., lipids, proteins, polysaccharides, DNA, etc.) secreted by autotrophic and heterotrophic microorganisms, responsible for the functionality and structural integrity of the biofilms [58,62]. The macromolecules (through dispersion forces, electrostatic interactions, and hydrogen bonds) create a gel-like substance around the cells, establishing a stable consortia of microorganisms [62]. Similar to the bacterial cell surface, EPS contains functional groups, including carboxyl, phosphoryl, amino, and hydroxyl groups [58,63,64]. These negative functional groups can attract positive divalent cations, thereby promoting precipitation of metal carbonate (MCO_3) compounds through local alkalization or inhibiting precipitation by removing the free cations from solution and reducing saturation. If the latter transpires, MCO_3 can be precipitated out of solution when EPS degrades and saturates solution with metal divalent cations [58,63]. The biochemical composition of EPS can affect the resulting mineralogy of $CaCO_3$, altering the polymorph (aragonite, vaterite, calcite) [65]. It can also alter the crystal morphology of $CaCO_3$ precipitates [66,67]. EPS is thought to influence the biofilm, cell adhesion, and capturing $CaCO_3$ precipitates [54]. Both EPS and biofilm formation can reduce pore space, increase ductility, increase strength, reduce hydraulic conductivity, and reduce permeability [68].

2.4. Microbial-Induced Carbonate Precipitation (MICP)

MICP is a complex process involving numerous metabolic pathways. These metabolic pathways can be enzyme-driven, redox-driven, or photosynthesis-driven reactions (Figure 2) [28]. Equations (3) and (4) illustrate the governing equations for calcium carbonate precipitation induced by biological processes [69]. The Ca^{2+} ion can be interchanged by other divalent cations to precipitate other MCO_3 compounds [45].

$$Ca^{2+} + Cell \rightarrow Cell - Ca^{2+} \quad (3)$$

$$Cell - Ca^{2+} + CO_3^{2-} \rightarrow Cell - CaCO_3 \quad (4)$$

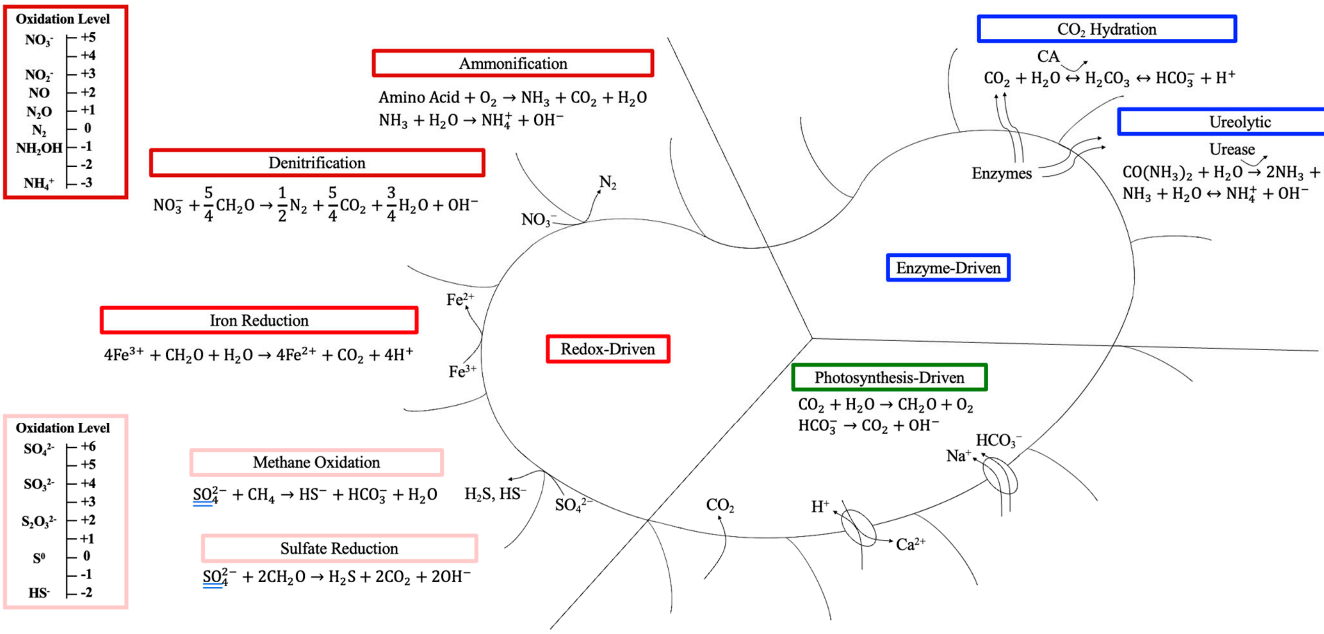

Figure 2. Biochemical reactions facilitating the different metabolic pathways of MICP, including redox-driven reactions (red), enzyme-driven reactions (blue), and photosynthesis-driven reactions (green). The reactions involved in the nitrogen (dark red) and sulfur (light red) cycle are highlighted. Adapted from [58,70].

Since SOC is considered energy limiting for microbial growth and carbonate mineralization [71], a nutrient broth (NB) is often added to supplement nutrient-deficient substrates for microbial growth. It is a complex concoction of chemicals and nutrients dependent on the desired microbial pathway. Nutrients often include carbon, nitrogen, and phosphorous, whereby an optimized ratio (C:N:P) is analyzed, typically approximately 100:10:1 [72]. The enzyme activity of urease, phosphatase, and dehydrogenase is involved in biogeochemical cycles of phosphate, nitrogen, and oxidation reduction of organic compounds and can illustrate the fertility of substrates [73].

Essential to MICP is a Ca^{2+} source. As mentioned above, Ca^{2+} concentration plays a vital role in $CaCO_3$ precipitation. Typically, a calcium source is added to facilitate precipitation. The most common calcium source used in research is calcium chloride ($CaCl_2$). The $CaCl_2$ compound undergoes dissolution, and the Ca^{2+} ions precipitate $CaCO_3$, while the chloride ions (Cl^-) form ammonium chloride (NH_4Cl), shown in Equation (5) [27,74]. However, calcium acetate ($C_4H_6CaO_4$) and calcium nitrate ($Ca(NO_3)_2$) are also used to facilitate carbonate precipitation [27]. Enhanced MICP is linked to higher concentrations of urea and $CaCl_2$ [75]. Stoichiometric calculations are required to determine the amount of urea necessary to convert all Ca^{2+} to $CaCO_3$ [76].

$$Cl^- + HCO_3^- + NH_3 \rightarrow NH_4Cl + CO_3^{2-} \tag{5}$$

The interaction of calcium with the microbial cell is an intricate process. The microorganism is surrounded by a thin layer of water, and when subjected to a low Reynold's number, protons (pH), DIC, and Ca^{2+} can concentrate in the microenvironment [52]. Ca^{2+} accumulates outside the microbial cell wall and is not likely utilized by the microbial metabolic processes [60]. McConnaughey and Whelan [77], Castanier [78], and Hammes and Verstraete [52], among other researchers, characterize the difference between "active precipitation" and "passive precipitation", whereby the former is linked to ion transport and exchange (specifically Ca^{2+}) through the cell membrane, and the latter encompasses precipitation via the metabolic pathways discussed below. Active precipitation is governed by calcium regulation via influxes and outflows (Figure 3). The transport mechanisms enabling active precipitation can be further classified as active or passive. Ca^{2+} influxes can be a passive transport mechanism based on the electrochemical gradient [52]. Concentrations of Ca^{2+} in the extracellular environment are typically 1000 times greater than in the intracellular environment due to low permeability of the cell envelope, high buffering capacities, and effective export mechanisms [79]. The passive transport mechanisms include antiporters ($Ca^{2+}/2H^+$, $Ca^{2+}/2Na^+$, etc.), protein-based channels, and non-proteinaceous channels. Active transport, however, includes Ca^{2+} transport against the electrochemical gradient using ATP-energy and ATP-dependent pumps [52].

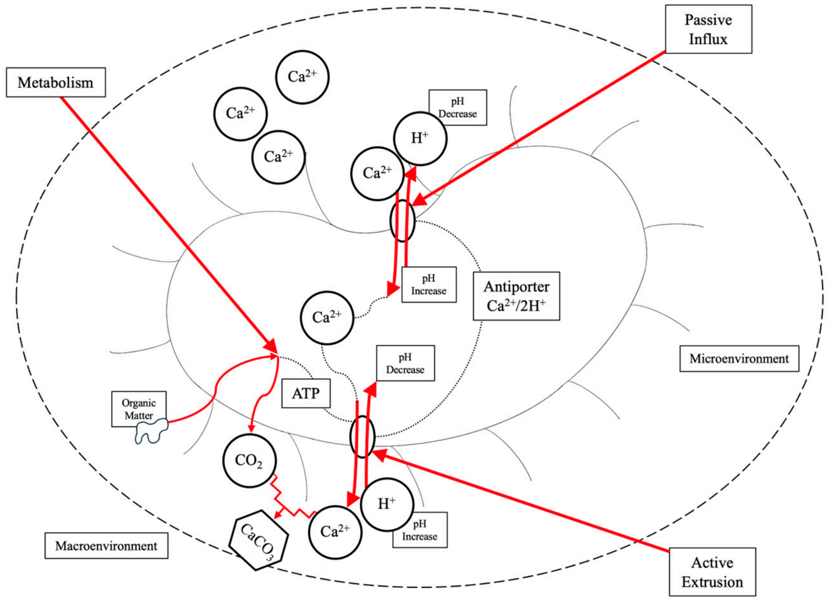

Figure 3. Calcium regulation in microorganisms showcasing the interaction and metabolism of calcium, leading to $CaCO_3$ precipitation. Adapted from [52].

The metabolism of calcium by the microorganism is a driving factor for $CaCO_3$ precipitation. In the microenvironment, when Ca^{2+} concentrations and pH (low H^+ proton concentration) are high in comparison to the microbial intracellular environment, the difference in electrochemical gradient will cause the $Ca^{2+}/2H^+$ antiporter to accumulate Ca^{2+} in the microbial cell and release H^+ protons to the extracellular environment. Through active extrusion, the microorganism will then release Ca^{2+} through ATP-dependent calcium pumps and uptake H^+ protons. This will create localized alkaline conditions and high Ca^{2+} concentrations ideal for precipitation. The metabolism of organic matter is required for ATP, which releases DIC to the extracellular environment in the form of CO_2. The CO_2 will undergo hydrolysis to form $HCO_3{}^-$ and $CO_3{}^{2-}$ ions (Equation (6)), which will interact with the Ca^{2+} ions and precipitate $CaCO_3$. This will impact the $CaCO_3$ solubility product. As the soluble Ca^{2+} ions decrease and there is an increase in acidity, the conditions become favorable for bacterial proliferation [52].

$$Ca^{2+} + HCO_3^- \rightarrow CaCO_3 + H^+ \tag{6}$$

2.4.1. Nitrogen Cycle

The nitrogen cycle plays a significant role in MICP. Three of the MICP metabolic pathways rely on the nitrogen cycle: denitrification, ammonification, and urea hydrolysis. In each of these scenarios, a pH increase ($NH_4{}^+$ and OH^-) in the presence of Ca^{2+} ions lead to $CaCO_3$ precipitation. Shown in Equation (2), a decrease in H^+ ions shifts the $CO_3{}^{2-}$–$HCO_3{}^-$ equilibrium to its $CO_3{}^{2-}$ form, inducing $CaCO_3$ precipitation [78].

Denitrification (Equation (7)) utilizes nitrate-reducing bacteria (NRB) to facilitate precipitation [58,80]. The dissimilatory reduction of nitrate ($NO_3{}^-$) increases pH through the consumption of $NO_3{}^-$ and the generation of OH^- ions [81]. Under anaerobic or hypoxic conditions, $NO_3{}^-$ acts as the electron acceptor producing inorganic carbon in the form of CO_2 [58,81]. Nitrogen (N_2) gas is an end product of dissimilatory nitrate reduction; however, intermediates include nitrite ($NO_2{}^-$), nitric oxide (NO), and nitrous oxide (N_2O) [82]. Toxic intermediates ($NO_2{}^-$ and N_2O) can accumulate if the involved enzymes are inhibited [58,83]. There are four enzymes involved in the denitrification process: nitrate reductase (Nar), nitrite reductase (Nir), nitric oxide reductase (Nor), and nitrous oxide reductase (Nos) [82]. The localization, lifetime, regulatory mechanisms, kinetics, and sensitivity to inhibitors are different for each of these enzymes, which can lead to incomplete denitrification at any of the reduction steps [83]. For example, nitrate or calcium overloading can cause inhibition, yielding the accumulation of toxic intermediates [83]. Synthesis of these enzymes is dependent on oxygen (O_2) concentration, pH, and temperature [84]. Evidence suggests nitrate plays a role in carbon-fixing pathways during carbon sequestration via revegetation, whereby nitrate directly impacts soil labile organic carbon and indirectly influences carbon-fixing microorganisms [85]. Furthermore, microbial genes identified in soils are involved in the nitrogen cycle and carbon fixation [86].

$$NO_3^- + \frac{5}{4}CH_2O \rightarrow \frac{1}{2}N_2 + \frac{5}{4}CO_2 + \frac{3}{4}H_2O + OH^- \tag{7}$$

Ammonification (Equation (8)) utilizes amino acids to produce NH_3 and $CO_3{}^{2-}$ via myxobacteria to induce precipitation [58]. *Myxococcus xanthus*, for example, is shown to induce precipitation of calcite and vaterite crystals [87–89]. This occurs under aerobic conditions with gaseous or dissolved oxygen and organic matter. These heterotrophic microorganisms use amino acids as an energy source and contribute to the degradation of organic matter [58,78]. The hydrolysis of NH_3 produces hydroxide ions (OH^-), creating a pH increase and leading to local supersaturation around the microbial cell, favoring precipitation [58]. Also formed from NH_3 hydrolysis is the $NH_4{}^+$ byproduct, often present in an aqueous state. $NH_4{}^+$ can easily convert into $NO_3{}^-$ and $NO_2{}^-$ [90], which can cause the accumulation of toxic nitrogen species in the environment. In addition, $NH_4{}^+$ in surface water can promote toxic algal bloom growth, impacting fish, flora, and fauna [91].

$$\text{Amino Acid} + O_2 \rightarrow NH_3 + CO_2 + H_2O \tag{8}$$

Urea hydrolysis involves the degradation of urea via ureolytic bacteria. The process consists of three main stages: (i) urea hydrolysis; (ii) pH increase; and (iii) cementation [69]. Ureolytic bacteria required for urea hydrolysis have a direct impact on the concentration of DIC (cell respiration and the decomposition of urea) and pH within the environment [58]. As part of the urea hydrolysis reaction (Equations (9) and (10)), 1 mol of urea ($CO(NH_2)_2$) via hydrolysis produces 1 mol carbamic acid (NH_2COOH) and 1 mol NH_3, where 1 mol NH_2COOH undergoes spontaneous hydrolysis to produce 1 mol NH_3 and 1 mol carbonic acid (H_2CO_3) [26,27,92]. This occurs via secretion of the enzyme urease (urea amidohydrolase; E.C. 3.5.1.5; nickel-containing metalloenzyme), which acts as a biological catalyst [93,94]. The enzyme speeds up the chemical reaction by lowering the activation energy via low-energy enzyme–substrate (i.e., urea) complexes. The bacteria use urease to hydrolyze $CO(NH_2)_2$ (added to the NB; NBU) by increasing ambient pH and using $CO(NH_2)_2$ as a nitrogen and energy source [60,93]. The NH_3 (Equation (11)) produced from enzymatic urea hydrolysis will again undergo hydrolysis to form $NH_4{}^+$ and OH^-, which increases pH [26,27,92]. The pH increases via urease can create a localized alkaline state in the microenvironment around the microbial cell, leading to $CaCO_3$ precipitation on or around the cell wall [60,74]. Urease production and subsequent $CaCO_3$ precipitation are impacted by the temperature, pH, concentration of $CO(NH_2)_2$, concentration of NH_3, carbon source, and incubation period [95].

$$CO(NH_2)_2 + H_2O \rightarrow NH_2COOH + NH_3 \quad (9)$$

$$NH_2COOH + H_2O \rightarrow NH_3 + H_2CO_3 \quad (10)$$

$$2NH_3 + 2H_2O \rightarrow 2NH_4^+ + 2OH^- \quad (11)$$

Through the precipitation of $CaCO_3$ is the development of cementation, which pertains to the large-scale precipitation in-between solid particles forming a biocement matrix [35,45]. It involves the dissociation of a calcium source into soluble Ca^{2+} ions [81], and an increase in $CO_3{}^-$ ions to reach the supersaturation state inducing $CaCO_3$ precipitation [69]. Again, $NH_4{}^+$ is produced as a byproduct. It should be noted that urea is very stable, and the purely chemical breakdown is independent of the pH between 2 and 12 [96]. The non-enzymatic process decomposes urea via elimination of NH_3 (half-life of 33 years at 25 °C) or spontaneous hydrolysis (half-life of 520 years at 25 °C) [97]. However, application of urease drastically increases the rate of reaction to a half-life in the microsecond range [97,98].

Several methods have been explored to reduce or remove harmful $NH_4{}^+$ byproduct from nitrogen-driven MICP pathways. These include flushing and extracting $NH_4{}^+$ with geophysical setups, electrokinetic retention of $NH_4{}^+$ in the cathode chamber of an electrokinetic cell, $NH_4{}^+$ precipitation via additives, and utilization of alternative metabolic pathways [99]. An alternative metabolic pathway is iron reduction utilizing iron-reducing bacteria [80,100]. Ferric iron (Fe^{3+}) acts as an electron acceptor in the presence of a carbon source, reducing to ferrous iron (Fe^{2+}) and CO_2 (Equation (12)) [80]. However, mineral precipitates are unstable and easily impacted by other ions [47]. Current research on this metabolic pathway is limited, although application of ureolytic MICP to iron-based substrates is emerging [101,102]. Iron-reducing bacteria have shown an impact in the complex coupling of Fe and C affecting carbon sequestration in paddy soils [103]. Furthermore, Fe can trap SOC via adsorption, coprecipitation [104], whereby ~21.5% of SOC is bound to reactive Fe phases in sediments [105].

$$CH_2O + 4Fe^{3+} + H_2O \rightarrow 4Fe^{2+} + CO_2 + 4H^+ \quad (12)$$

The efficacy of the urease enzyme can be impacted by nickel. The urease enzyme is composed of structural genes and accessory genes in operons and clusters [26,106]. Inactive urease (apo-urease) has structural genes (*ureA*, *ureB*, and *ureC*) requiring accessory genes (*ureD*, *ureF*, *ureG*, and *ureE*) for activation. Activation involves CO_2 uptake for lysine carbamylation, hydrolysis of guanosine triphosphate (GTP), and Ni^{2+} delivery to its active site [107]. As mentioned preciously, nickel is incorporated in the active center of urease [26] and contains two nickel ions (Ni^{2+}) bridged by a hydroxyl group and a carbamylated lysine [108]. The *ureE* gene, specifically, is responsible for delivering Ni^{2+} to the active site, leading to fully active urease (holo-urease) and subsequent urea hydrolysis [107]. A mobile flap (from the helix-turn-helix motif) covers the active site, restricting access [109]. As shown in Figure 4, ureolysis occurs when the flap is open and urea enters the active site, replacing water molecules bound to Ni^{2+} ions. The C-O bonds in urea are polarized and undergo nucleophilic attack because of the highly electrophilic Ni ions with the bridging OH [107,109,110]. The NH_2 is protonated by the bridging Ni OH (or His320, Ala167, Ala363, Cys319, His219, G277) [110], and the C-N bond is broken, releasing NH_3 [107,109]. The carbamate ($CH_2NO_2{}^-$) remaining decomposes further (Equation (13)), and all products are released with the flap opening [107]. Furthermore, urease inhibition is attributed to Ni^{2+} binding, which leads to a loss in urease and catalytic activity. This includes impacts to the direct binding of Ni^{2+} at the active urease sites; covalent modifications that cover the Ni^{2+} center; and metal ion chelators that sequester Ni^{2+}, thereby inhibiting the formation of the Ni^{2+} center [108]. Ni^{2+} in the form of nickel chloride ($NiCl_2$) and nickel nitrate ($Ni(NO_3)_2$) has been added to the NB to enhance $CaCO_3$ precipitation [111,112]. In addition to ureolysis, nickel is involved in hydrogen metabolism and methane biogenesis, and acts as an essential nutrient to microorganisms [109].

$$NH_2COO^- + 2H_2O \rightarrow NH_4^+ + HCO_3^- + OH^- \quad (13)$$

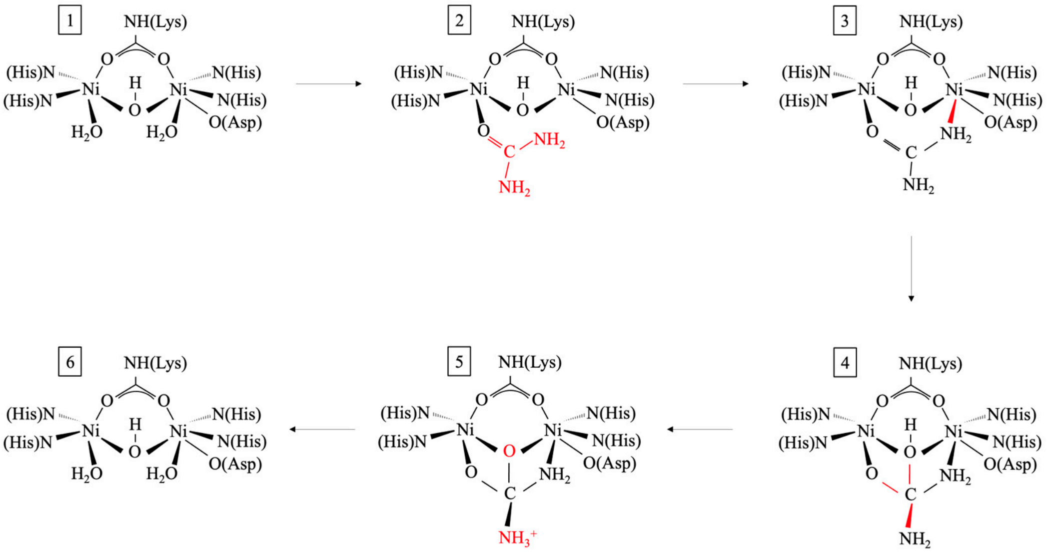

Figure 4. Simplified schematic of the structure-based reaction mechanism of urease. Red indicates the changes step by step. The flap is open (1), and urea enters the activated site, replacing water and binding to carboxyl oxygen (2). The flap closure enables urea binding to Ni^{2+} (3). The carbon atom on urea undergoes nucleophilic attack via Ni^{2+} bridging OH, creating a tetrahedral intermediate (4). The Ni bridging OH transfers the hydrogen atom to the distal urea NH_2 group, forming NH_3^+ (5). The distal C-N bond is broken, and all products are released via a flap opening, which rehydrates the active site (6). Adapted from [108,111].

Application of ureolytic MICP for carbon sequestration showed efficacy ≤86.4%, dependent on the bacterial community structure and pH [113]. Higher-headspace CO_2 uptake was shown with *Sporosarcina*, *Sphingobacterium*, *Stenotrophomonas*, *Acinetobacter*, and *Elizabethkingia* species [113]. An increase ≤ 148.9% in CO_2 uptake through calcification can be shown in optimal urea growth media [33]. Conversely, ureolytic bacterial growth utilizing *Bacillus megaterium* demonstrated comparable quantities of precipitated $CaCO_3$ with 99.5% pure CO_2 influx to that of 2% NBU [114].

2.4.2. Sulfur Cycle

The sulfur cycle also plays an interesting role in MICP (Equation (14)). In sulfate (SO_4^{2-})-rich environments, sulfate-reducing bacteria (SRB) facilitate either dissimilatory or assimilatory sulfate reduction, producing hydrogen sulfide (H_2S) or organic sulfur (S), respectively [115,116]. This reaction transforms organic carbon in the form of an energy source to HCO_3^-, and will release OH^- and increase alkalinity, leading to a supersaturation state and therefore the likelihood of CO_3^{2-} precipitation [58]. SRB (comprising 87% *Halanaerobiaceae*, *Halobacteroidaceae*, *Enterobacteriaceae*) have been enriched from sediment samples for carbon sequestration, whereby ~53% of precipitated carbonate minerals are derived from CO_2 headspace [117]. In this study, headspace pressure played an integral role in carbonate precipitation at ≤ 14.7 psi [117]. The SRB can also degrade EPS, releasing trapped Ca^{2+} into the environment, leading to $CaCO_3$ precipitation [58]. Further, the H_2S produced during the reaction may subsequently degas, increasing pH, increasing precipitation, or being utilized by bacteria [78]. However, the H_2S can be highly toxic [81], and if not degassed or if unused by bacteria, it can cause pH to decrease and inhibit precipitation [78]. The process is most prominent under anaerobic or anoxic conditions rich in organic matter [26,78]. Sulfate reduction contributes ~36–50% carbon mineralization in anaerobic wetlands [118] and plays a significant role in stromatolite formation [119].

$$SO_4^{2-} + 2CH_2O \rightarrow H_2S + 2CO_2 + 2OH^- \tag{14}$$

Methanogens also utilize ${SO_4}^{2-}$ to induce methane oxidation [58]. Under anaerobic conditions, methane oxidation favors carbonate precipitation (Equation (15)), while aerobic conditions increase alkalinity, favoring carbonate dissolution (Equation (16)) [58,120]. Both scenarios can facilitate carbonate precipitation in the presence of a divalent cation source (i.e., Ca, Fe, Mg, Mn, Ba) [121]. However, interesting is the removal of CH_4 emissions and its application as a methane sink offsetting GHG emissions [122]. The process transforms CH_4 to a less toxic form and locks carbon as mineral precipitates. Furthermore, in situ anaerobic carbonate precipitation via methane oxidation can be subdivided into sulfate-dependent precipitation in shallow sediments or marine silicate weathering in deep sediments [121]. Unlike the other metabolic pathways that are solely heterotrophic, methane oxidation can be both an autotrophic [26,123] or heterotrophic process [124]. It can also use alternative electron sources to ${SO_4}^{2-}$, including ${NO_3}^-$, ${NO_2}^-$, Fe, Mn, and humic acid [120]. While methane oxidation in terms of MICP is often neglected in experimental research, a recent study has identified methanogenesis as a metabolic pathway in activated anaerobic sludge [99].

$$SO_4^{2-} + CH_4 \rightarrow HS^- + HCO_3^- + H_2O \tag{15}$$

$$2O_2 + CH_4 \rightarrow CO_2 + 2H_2O \tag{16}$$

2.4.3. Photosynthesis

Purely autotrophic pathways (i.e., non-methylotrophic methanogenesis, anoxygenic photosynthesis, and oxygenic photosynthesis) utilize gaseous or dissolved CO_2 from the atmosphere, respiration, or fermentation [78]. This CO_2 acts as their carbon source to produce organic matter and, under Ca^{2+} rich environments, can favor $CaCO_3$ precipitation [78]. Photolithoautotrophs, specifically, cyanobacteria, have been studied for their capacity for carbonate biomineralization [120], with their higher affinity for environment CO_2 due to photosynthesis and CO_2 fixation by the Calvin cycle [125]. Approximately 70% of carbonate rock in the history of Earth is contributed to cyanobacteria [126]. Cyanobacteria carbonate mineralization occurs in four steps: (i) $CO_2/{HCO_3}^-$ uptake for photosynthesis; (ii) OH^- release; (iii) OH^- and ${HCO_3}^-$ reaction forming ${CO_3}^{2-}$; (iv) carbonate precipitation [127]. The CO_2 (Equation (17)) enters the cell wall via diffusion or a symporter, where CO_2 produces organic matter utilized by the microorganisms [58]. ${HCO_3}^-$ (Equation (18)) is transported from the extracellular environment into the cell membrane, which dissociates into CO_2 and OH^- [26]. ${HCO_3}^-$ is the predominant form of inorganic carbon transported into the cell [127]. The OH^- ion is released from the cell to the extracellular environment, increasing pH, which again favors $CaCO_3$ precipitation in Ca^{2+}-rich environments [26,58]. The equilibrium reached between ${HCO_3}^-$ into the cell and the efflux of OH^- from the cell causes the alkalinization in the microenvironment around the cell [127]. $CaCO_3$ nucleation occurs on the sticky cell walls of cyanobacteria, which aid in binding [128]. Furthermore, calcium metabolism can store Ca^{2+} within the cell membrane, precipitating $CaCO_3$ intracellularly, or can release Ca^{2+} through the $Ca^{2+}/2H^+$ antiporter, precipitating $CaCO_3$ extracellularly [58]. This process has been investigated more frequently due to the nature of its less harmful byproduct (CH_2O). The absence of ${NH_4}^+$ or H_2S make this pathway desirable. Naturally occurring photosynthesis-driven carbonate mineralization is shown in karstic environments to offset mine-related GHG emissions by ~20% [129,130].

$$CO_2 + 2H_2O \rightarrow CH_2O + O_2 \quad (17)$$

$$HCO_3^- \rightarrow CO_2 + OH^- \quad (18)$$

Carbonic anhydrase (CA; EC 4.2.1.1; zinc-containing metalloenzyme) is an enzyme-driven metabolic pathway essential for carbon sequestration [34,93]. The enzyme catalyzes the reversible hydration of CO_2 (Equation (2)) and plays a role in pH regulation [120]. The enzyme is very complex, containing five distinct classes (α, β, γ, δ, and ε; evolutionarily independent) [131], and α-CA contains 15 isozymes [132]. The enzyme can be intracellular, intra-organellar, periplasmic, or extracellular [120]. Intracellular CA can possess a carbon-concentrating mechanism (CCM) to capture and sequester CO_2 [131,133,134]. Inorganic-carbon-concentrating mechanisms (Figure 6) can occur from (i) diffusion or active transport of carbon (CO_2 or ${HCO_3}^-$) across the cytoplasmic membrane via energy-dependent transporters; (ii) CA conversion to ${HCO_3}^-$, which accumulates in the carboxysome; (iii) conversion of ${HCO_3}^-$ back to CO_2 by CA, which concentrates and fixes elevated concentrations of CO_2 in the Rubisco [125,133]. The CCM is thought to have evolved from the decline of atmospheric CO_2 and increase in O_2 in the Phanerozoic era, triggering oxygenic photosynthesis in cyanobacteria [135]. The CCM genes (ccmK, ccmL, ccmM, ccmN, and ccmO) enable growth at low pCO_2 for assembly in the carboxysome [125]. The carboxysome (sub-cellular compartment encapsulating Rubisco and CA) is a primary component of CCM [136]. There exists a differentiation between α-cyanobacteria and β-cyanobacteria based on the type of carboxysome and Rubisco [135]. The carboxysome is separated into α-carboxysome and β-carboxysome, both of which limit CO_2 leaching; reduce the risk of photorespiration; and enhance carboxylase, the activity of Rubisco [136]. The CA enzyme is specific to the type of carboxysome: α-carboxysome requires β-CA (CsoSCA), and β-carboxysome requires β-CA (CcaA) and γ-CA (CcmM) [136,137], but β-CA has a direct involvement in CCM of β-cyanobacteria [135]. β-cyanobacteria also contain non-carboxysomal CA localized in the cell membrane or periplasmic space: α-CA (EcaA) and β-CA (EcaB) [136]. Cyanobacteria have been identified in hot/cold, alkaline/acidic, marine, freshwater, saline, terrestrial, and symbiotic environments [138]. The CCM of α-cyanobacteria and β-cyanobacteria is dependent on their environmental conditions (i.e., pH, carbon content, salinity, temperatures, oxygen content, light, wet/dry conditions) [138]. However, pH is most prominent since it is linked to carbon speciation (i.e., H_2CO_3, CO_2, ${HCO_3}^-$, ${CO_3}^{2-}$) [136].

However, α-CA are localized in the periplasmic or extracellular space, and it is hypothesized that they are able to convert diffused CO_2 into ${HCO_3}^-$ for bacterial metabolism [139]. Extracellular α-CA has been identified from prokaryote *Pseudomonas fragi* [140], *Bacillus* sp. [131], cyanobacteria *Microcoleus chlthonoplastes* [141], *Bacillus mucilaginosus* [142]. Both intracellular and extracellular CA could be detected in soil bacteria, whereby some CA was absorbed by soil [143]. The extracellular CA likely stabilizes the pericellular pH and induces carbonate precipitation [141] at or near the bacterial cell wall.

While nickel is at the core of urease, CA contains a zinc core [144]. The zinc plays a vital role in the CA activity [145]. There are several genetically distinct forms of CA, each containing a catalytically obligatory zinc ion (Zn^{2+}) [146]. The hydrogen bonding network stabilizes the electrostatic environment of zinc, impacting catalytic efficacy [147]. The structure of CA (Figure 5) and orientation of CO_2 enhance the likelihood of nucleophilic arrack of the Zn^{2+}-bound water molecule. This leads to HCO_3^- formation, which is subsequently replaced by a water molecule, releasing HCO_3^- from the active site [148]. The addition of zinc as zinc sulfate ($ZnSO_4$) can have a positive effect on CA activity [144]. However, studies show that the zinc ion in the enzyme is firmly bound to the protein, forming a stable metal–protein complex, and therefore, ion exchange with Zn^{2+} in solution is unlikely [149]. CA inhibition can occur via bonding to the zinc-coordinated water molecule/hydroxide ion [134]. This can occur via metal complexing anions and substitution of the non-protein zinc ligand [148].

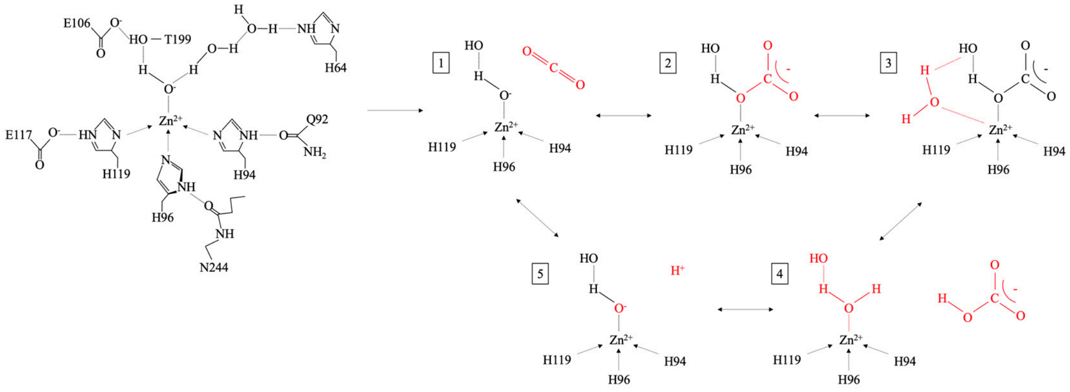

Figure 5. Simplified schematic of the structure-based reaction mechanism of CA. CA II active site structure (**left**) and reaction (**right**). The Zn-bound OH^- attacks the carboxyl carbon of CO_2 (1), creating Zn-bound HCO_3^- (2). A water molecule (3) replaces the HCO_3^- bound to Zn (4), and H^+ is transferred to solution (5). Adapted from [146,150,151].

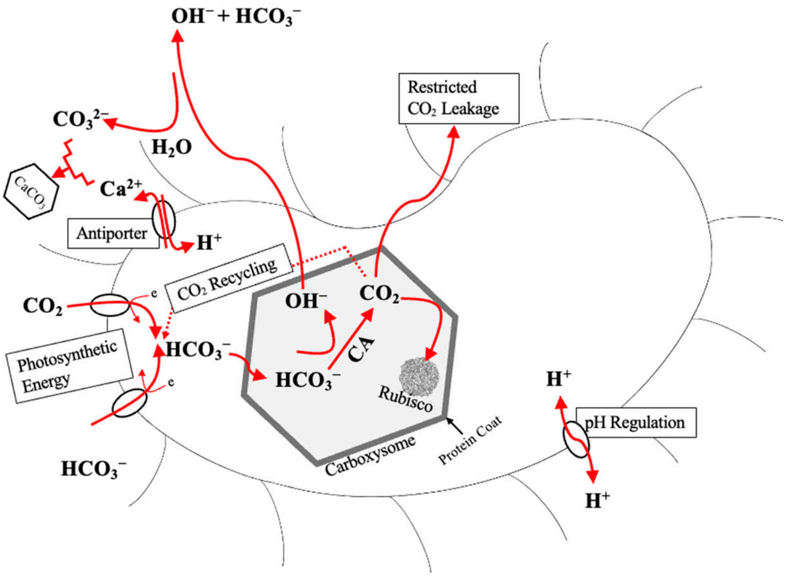

Figure 6. A generic model of the CCM of cyanobacteria showing accumulation of HCO_3^- in the cytosol, Rubisco-containing carboxysome, and CA. Intracellular pH is buffered via Ca^{2+}/H^+ antiporter, which alone releases OH^- in the extracellular environment and increases pH, favoring extracellular $CaCO_3$ precipitation. Adapted from [124,138,140,142].

The enzyme-driven pathways (urease and CA) can be independent processes, but they can also work synergistically to facilitate carbon sequestration [54,93,152]. CO_2 dissolution can decrease pH due to proton enrichment [21,153]. However, there will also be a pH increase from NH_4^+ from urea hydrolysis [154], which maintains the alkaline state required for precipitation [93]. Further, the urease enzyme has nickel incorporated in the active center, and an increase in CO_2 (regulated by CA) is shown to generate ligands for nickel binding, which is essential to urease activity [26,155]. The nickel core is dependent on CO_2/HCO_3^- metabolism [93]. However, it should be noted that carbon sequestration can occur independently as a purely chemical reaction [33], whereby CO_2 is dissolved in water, converted to CO_3^{2-}, and then precipitated as $CaCO_3$ without biological interference.

3. Carbon Sequestration

Carbon sequestration methods are characterized as direct (i.e., involved in reduction in CO_2 emissions by sequestering inorganic carbon prior to atmospheric release) or indirect (i.e., reliance on natural carbon sinks) [41]. The direct methods require CCS techniques for CO_2 removal, which includes absorption (chemical, physical), adsorption (adsorber beds, regeneration methods), cryogenics, membranes (gas separation, gas absorption, ceramic-based systems), and microbial/algal systems [41]. Mechanisms for carbon sequestration are outlined in Figure 7.

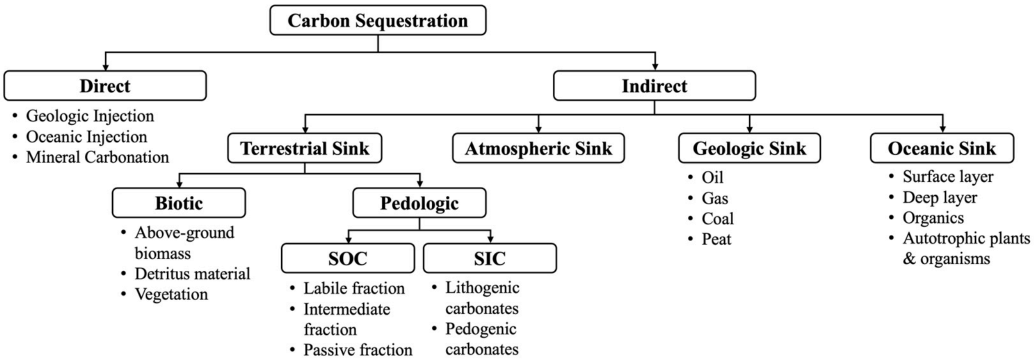

Figure 7. Direct and indirect carbon sequestration methods. Adapted from [40,41,156].

As shown in Figure 7, there are 4 major carbon pools responsible for indirect carbon sequestration. A carbon pool refers to a system that can accumulate or release carbon [157], and these include oceanic, geologic (fossil fuels i.e., coal, oil, gas, peat), terrestrial (pedologic (i.e., SOC, soil inorganic carbon (SIC)) and biotic (i.e., vegetation), and atmospheric pools [40]. A major factor in the global warming crisis is the depletion of fossil fuel carbon pools and the anthropogenic release of GHGs back into the atmosphere. The majority of GHGs are released by the combustion of fossil fuels for energy and transportation. Current methods of carbon sequestration are typically defined as abiotic (oceanic injection, geologic injection, mineral carbonation) or biotic (oceanic sequestration, terrestrial sequestration, mineral carbonation) processes [40].

Oceanic carbon sequestration can be both an abiotic and biotic process. These techniques rely on the solubility pump and autotropic mechanisms [41]. Methods can stimulate growth of autotrophic organisms (phytoplankton, microalgae, macroalgae, and cyanobacteria) on the ocean surface to enhance photosynthesis to remove atmospheric CO_2 [41]. The methods can utilize DOC for: (i) photosynthesis; (ii) remineralization; (iii) assimilation by microorganisms [158]. The trapped carbon via biological carbon pumps (i.e., gravitational settling, ocean mixing and animal migrations) to mobilize the organic matter downward for burial at the ocean bottom [159,160]. Alternatively, CO_2 can be injected in liquified phase directly into the deep ocean (> 1 km) to form CO_2 hydrate for permanent storage [161].

Deep geologic injection, as named, involves deep geologic injection of supercritical CO_2 into porous aquifers (i.e., coal seams, oil beds, deep saline aquifers) capped by low permeability rock [162]. The CO_2 can be trapped by: (i) mineral trapping through precipitation of carbonate minerals; (ii) geologic trapping by physical containment in geologic features; (iii) solubility trapping via dissolution in liquid; (iv) hydrodynamic trapping from CO_2 and liquid viscosity differences; (v) capillary trapping due to capillary forces; (vi) sorption of CO_2 on the materials surface [21]; (vii) formation trapping by reduced geologic permeability to reduce CO_2 leakage [53]. In saline aquifers, the CO_2 injected in supercritical state can be sequestered hydrodynamically by reacting with dissolved salts forming carbonate minerals, by an additive of lower density. The lower viscosity solution displaces brine, which creates a multiphase (gas-like and aqueous) environment [40]. Sedimentary basins are well suited for CCS via deep geologic injection due to the high pore volume and connectivity [163].

3.1. Mineral Carbonation and Carbon Sequestration

Mineral carbonation is significant to both abiotic and biotic carbon sequestration methods. The method can be naturally occurring mimicking the natural weathering process of alkaline silicates (Equations (19)–(21)) [164]. The process dissolves atmospheric CO_2 in rainwater to process weak carbonic acid (H_2CO_3), which is slightly acidic causing metal ions to leach from natural alkaline silicates neutralizing their mineral alkalinity and precipitating of carbonates [164]. The process precipitates geologically, geochemically and thermodynamically stable carbonate precipitates [40,164,165]. These precipitates are low solubility [166], and would require acidic conditions or high temperatures (~900 °C) to release CO_2 from the mineralized precipitate [167]. Mineral carbonation is therefore considered permanent solution for carbon sequestration of atmospheric CO_2 [168]. Carbonation is impacted by: solid to liquid ratio, particle size, temperature, ion transport mechanisms [166], pH, crystal ageing, agitation, and impurities [169]. It should be noted that environments with high pH leachate from weathering with high $CaCO_3$ precipitation can: (i) smother benthic ecosystems; (ii) damage littoral aquatic habitats; (iii) reduce light penetration to benthic primary producers; and (iv) harm fish populations [170].

$$CaSiO_{3(s)} + 2CO_{2(aq)} + H_2O_{(l)} \rightarrow Ca^{2+}{}_{(aq)} + 2HCO_3^-{}_{(aq)} + SiO_{2(s)} \tag{19}$$

$$MgSiO_{4(s)} + 4CO_{2(aq)} + 2H_2O_{(l)} \rightarrow 2Mg^{2+}{}_{(aq)} + 4HCO_3^-{}_{(aq)} + SiO_{2(s)} \tag{20}$$

$$(Mg^{2+}, Ca^{2+})_{(aq)} + CO_3^{2-}{}_{(aq)} \rightarrow (Mg, Ca)CO_{3(aq)} \rightarrow (Mg, Ca)CO_{3(s)} \tag{21}$$

Accelerated carbonation is a process used to replicate the natural weathering process. It speeds up the process by utilizing high-purity CO_2, which reacts with alkaline materials in the presence of moisture to precipitate carbonates within minutes or hours [171]. There are two main categorizes of processes: the direct method (single reaction step) and the indirect methods (alkaline metal ions are extracted prior to carbonate precipitation in a multi-step process) [164,165,172]. A primary advantage of indirect processes is the production of pure $CaCO_3$ (or $MgCO_3$) without impurities (i.e., silica) [173]. The process can further be classified as in-situ or ex-situ approaches [174,175]. The former injects CO_2 directly into the porous material to react with the host rock, whereas the latter uses industrial chemical processes to carbonate natural minerals and industrial waste in treatment plants [174]. Interestingly, the use of alkaline waste originates from industrial and mining activities as host rock for carbon sequestration [165,166,172,176], whose operations and feedstock are often located near point-source GHG emission sources [175]. The operations are promising for storage of atmospheric CO_2 as carbonate precipitates and offsetting CO_2 emissions from high-GHG producers. Natural CO_2 sequestration has been demonstrated in chrysotile mine tailings in Clinton Creek, YT and Cassiar, BC, whereby the process is accelerated by the increased surface area from milling [177]. Researchers have also incorporated CA into accelerated mineral carbonation of alkaline brucite ($Mg(OH)_2$) to overcome the carbonation rate-limiting supply of CO_2, demonstrating acceleration of 240% over controls [178].

Direct mineral carbonation methods (Table 3) can be gas-solid carbonation or aqueous carbonation (gas-liquid or gas-liquid-solid) [164]. The operation is simple relying on an input of CO_2 to facilitate precipitation of carbonate minerals. Direct precipitation can occur under dry or moist conditions [164]. However optimal CO_2 sequestration often requires a degree of moisture [179–182]. The particle size also plays an important role, whereby smaller particle sizes are preferable [180,183]. Mechanical pretreatment (crushing and grinding) can be used to reduce particle size <300 µm, destroying the mineral lattice and increasing surface area for the reaction [175]. Researchers are also studying thermal pre-treatment, NETL derived processes, brine-based processes, and organic acid direct processes [175]. Although these processes can be considered indirect stepwise gas-solid methods [184]. Fagerlund et al. [185], for example, are studying stepwise carbonation of serpentinite (Equations (22) and (23)) at Åbo Akademi University, whereby magnesium ions are released from $Mg_3Si_2O_5(OH)_4$ through heat (400–500 °C) and ammonium sulphate ($(NH_4)_2SO_4$) induce precipitation of magnesium sulfate ($MgSO_4$), which afterwards is used to precipitate magnesium hydroxide ($Mg(OH)_2$) via an aqueous ammonium hydroxide solution (NH_4OH). The $Mg(OH)_2$ precipitate is then used for carbonation with CO_2 injection to precipitate $MgCO_3$.

$$Mg_3Si_2O_5(OH)_4 + 3\,(NH_4)_2SO_4 \rightarrow 3MgSO_4 + 2SiO_2 + 5H_2O_{(g)} + 6NH_{3(g)} \tag{22}$$

$$MgSO_4 + 2NH_4OH_{(aq)} \rightarrow (NH_4)_2SO_{4(aq)} + Mg(OH)_2 \tag{23}$$

Table 3. Direct methods for mineral carbonation and carbon sequestration.

Method	**Material**	**CO_2 Application**	**CO_2 Input [1]**	**Results [1]**	**Findings**	**Reference**
Direct Gas–Solid Carbonation	Municipal Solid Waste Incinerator	CO_2 flow	100% CO_2, 3 bars, 2.5 h	3.19% $CaCO_3$ gain bottom ash 7.31% $CaCO_3$ gain fly ash	More suitable to small particle size.	[183]
			100% CO_2, 3 bars, 3 h	11% $CaCO_3$ gain fly ash	Optimal CO_2 capture at water/solid ratio 0.3.	[179]
			17 bars, 3 h	3% $CaCO_3$ gain bottom ash	Optimal CO_2 capture 20% *w*/*w* moisture and 4 mm sieving.	[180]
			1 bar, 1 h	60 g CO_2/kg fly ash	Temperature (600 °C) and $H_2O_{(g)}$ (20%) are more significant than CO_2 content.	[181]

Table 3. *Cont.*

Method	Material	CO_2 Application	CO_2 Input [1]	Results [1]	Findings	Reference
	Waste Concrete & Anorthosite Tailings		18.2 vol% CO_2, 4 & 5 bar, 30 min	66% CO_2 removal waste concrete 34% CO_2 removal anorthosite	Aqueous phase carbonation resulted in 34.6% removal in 15 min.	[186]
	Pre-treated EAF steel-making bag house dust		3 bar inlet, 1 bar (outlet), 12 L/min	0.657 kg CO_2/kg dust	Carbonation was based on the total calcium content.	[187]
	Air Pollution Control Residues from a Medical Solid Waste Incinerator		100% CO_2, 6 h	0.12 kg CO_2/kg dry solid waste	Maximum carbonation at 400 °C.	[188]
	Serpentinite Mining Residue	CO_2 concentration	18 vol% CO_2	0.07 g CO_2/g residue	Water vapor (10 vol%) required for carbonation.	[182]
Direct Aqueous Carbonation	Concrete Fines	CO_2 flow	14% CO_2, 90 min	0.19 g CO_2/g concrete fines	Almost all absorbed CO_2 was converted to $CaCO_3$, and increased CO_2 concentration requires higher solid–liquid ratio.	[189]
	Olivine with $NaHCO_3$ & NaOH Buffers		pCO_2 6.5 MPa, 6 h	<80% carbonation	Agitation is necessary to prevent solids settlement. Low pCO_2 requires high $NaHCO_3$ concentration.	[190]
	Flue Gas Desulfurization Gypsum		1 L/min, 15 min	90% $CaCO_3$ efficiency	$CaCO_3$ precipitation increased linearly with ammonia content.	[191]
	Steel Slag		19 bar CO_2, 30 min	0.25 kg CO_2/kg steel slag	Primary factors: particle size <2mm to <38 µm and temperature 25–225 °C.	[192]

Table 3. *Cont.*

Method	Material	CO_2 Application	CO_2 Input [1]	Results [1]	Findings	Reference
	Red-Mud	CO_2 concentration	3.5 bar, 3.5 h	5.3 g CO_2/100 g red mud	At liquid–solid ratio of 0.35.	[193]
	Oil Shale Ash		Continuous flow (0.7 m/10 L), 15% CO_2	17–20% bound CO_2	Size and structure of $CaCO_3$ depended on end-point pH.	[194]
	Coal Fly Ash		10 bars, 18 h	26 kg CO_2/ton fly-ash	Pressure was independent of carbonation efficiency and not affected by temperature of fly ash weight.	[195]
	Industrial/ Mining Wastes		15% CO_2	544.6 g CO_2/kg carbide slag	Ca content in material produces increased carbonation. Max carbon sequestration occurred at < 75 µm particle size, 60 °C, 100 g/L liquid–solid ratio.	[196]
	Aggregate Recycling Concrete Fines		5% CO_2	0.13 g CO_2/g concrete fines	0.10 CO_2/g concrete fines captured as $CaCO_3$, and 0.02 CO_2/g concrete fines dissolved in aqueous.	[197]
	Low-Calcium Fly Ash		30% CO_2	0.016 g CO_2/g fly ash	Good carbonation potential despite low energy input and low calcium content.	[198]

[1] As reported in the literature.

Alternatively, the direct aqueous method relies on the reaction of CO_2 and water (Equation (2)) to form HCO_3^- and a proton (H^+), which releases the divalent cation from the mineral (Equation (24)) to precipitate carbonate (Equation (25)) [199]. The reactions can be accelerated more via additives (i.e., bicarbonate/salts, acids, or chemical activators) or pretreatment methods (comminution, magnetic separation, heat treatment), which alter reaction conditions and modify solution chemistry to increase reaction rates to increase carbonate precipitation [172].

$$MgSiO_4 + 4H^+ \rightarrow 2Mg^{2+} + SiO_2 + 2H_2O \quad (24)$$

$$Mg^{2+} + 2HCO_3^- \rightarrow MgCO_3 + H^+ \quad (25)$$

Indirect mineral carbonation typically utilizes stepwise gas-solid, pH swing, or chemically enhanced mechanisms [184]. In the former, acid addition is utilized to enforce metal separation and a base additive induces aqueous carbonation [164,184]. The latter, chemically enhanced mechanisms, can include: HCl extraction, the molten salt process, other acid extractions (acetic acid (CH_3COOH), sulfuric acid (H_2SO_4), nitric acid (HNO_3), and formic acid (HCOOH)), bioleaching, ammonia extraction, and caustic extraction [172]. Acid extraction merely extracts the desirable metals from mineral prior to aqueous carbonation [164], causing potentially unfavorable conditions for precipitation (i.e., acidic conditions cause low CO_2 dissolution and the low pH inhibits precipitation) [172]. HCl extraction, for example, showed no precipitated $CaCO_3$ due to the rapid pH decline causing acidic conditions inhibition precipitation [200]. The pH swing process was developed by Park and Fan [201] to overcome these limitations. Wang and Maroto-Valer [202] have developed an amended pH swing method for serpentine incorporating the following steps: (i) CO_2 is captured and reacts with NH_3 to form NH_4HCO_3 intermediary; (ii) mineral dissolution via NH_4HSO_4 additive producing $MgSO_4$; (iii) NH_4OH is added to neutralize pH and remove impurities; (iv) $MgSO_4$ reacts with NH_4HCO_3 at mild temperature to form $Mg(HCO_3)_2$ converting in the presence of water to $MgCO_3$; (v) recovery of $(NH_4)_2CO_3$ from carbonation via evaporation and heating to produce NH_4HSO_4 and NH_3 for reuse.

Bioleaching utilizes byproducts (i.e., production of organic acids, chelating and complexing compounds) excreted by microorganisms to extract metals from minerals [203]. The humic and organic acids, inorganic acids, and chelating agents can free nutrients enhancing physical and chemical weathering [204]. These steps can be categorized by direct (Equation (26)) or indirect (Equation (27)) bacterial leaching, whereby both equations show metal sulfide (MS) oxidation into metal sulfate (MSO_4) [203]. In Equation (26), bacterial enzyme activity catalyzes the mineral sulfate oxidation through direct physical contact between the bacterial cell and the mineral sulfide surface [203]. Metal sulfides include: covellite (CuS), chalcocite (Cu_2S), sphalerite (ZnS), galena (PbS), molybdenite (MoS_2), stibnite (Sb_2S_3), cobaltite (CoS), millerite (NiS), and pyrite (FeS_2) [203]. The indirect oxidation in Equation (27), is generated by a catalytic function of a lixiviant which chemically oxidizes the sulfides [203]. In both scenarios, potentially acid generating substances (i.e., comprising sulfides or elemental sulfur) provide food for bacteria, which generated sulfuric acid as a by-product of metabolism, which leaches metals from minerals [172]. Furthermore, autotrophic bacteria (i.e., chemolithoautotrophic) can fix carbon biologically through the process by utilizing inorganic, atmospheric CO_2 instead of organic carbon for new cell synthesis [172,203]. Factors influencing bioleaching include nutrients, O_2 and CO_2 content, pH (acidic conditions), temperature, mineral substrate (dependent on mineralogical composition and particle size), heavy metals, surfactants and organic extractants (decrease surface tension and mass transfer or oxygen) [203]. Chiang et al. [205] attributed bioleaching to organic acid production, specifically gluconic acid ($C_6H_{12}O_7$), and microbial exopolysaccharides (EPSs). Similar to other mineral carbonation techniques, the released metal ions are available for carbonate precipitation. Bioleaching of ultramafic mine tailings can be used at tailings storage facilities [206]. Chrysotile tailing indicate acid mine drainage environments with microbial catalyst from *Acidithiobacillus* sp. is promising for $MgCO_3$ precipitation with atmospheric CO_2 resulting in 316 kt Mg leached/10 Mt tailings (458 kt CO_2 sequestered/year) [207]. Argon Oxygen Decarburization slag showed a decline in primary phase (dicalcium-silicate, bredigite, and periclase) and an increase in secondary phases (merwinite and calcite), specifically a 3.1 wt % increase in $CaCO_3$ with *B. mucilaginous* bacterial species [205].

$$MS + 2O_2 \overset{\text{Bacteria}}{\rightarrow} MSO_4 \tag{26}$$

$$MS + Fe_2(SO_2)_3 \rightarrow MSO_4 + 2FeSO_2 + S^0 \tag{27}$$

3.2. Advancements to Mineral Carbonation for Carbon Sequestration

Microbial carbon mineralization has a unique opportunity to utilize novel biochemical mechanisms for carbon sequestration. The process can sequester inorganic carbon as a CCS technique via carbonate precipitation, but also mitigate CO_2 released to the atmosphere therefore reducing atmospheric CO_2 levels to aid the impacts of climate change [208]. The MICP enzyme-driven reactions speed up chemical reactions to enhance the rate of reaction and therefore conversion to $CaCO_3$, optimizing storage of inorganic CO_2. The synergistic role of CA and urease enzymes work to hydrate atmospheric CO_2 while inducing an alkaline state for biocalcification [93]. Again, alkaline material is a preferential substrate for carbon sequestration [165,166,172,176], therefore halotolerant and alkalophilic bacteria are required for biocalcification. Ureolytic bacteria offer a preferable metabolic pathway for MICP, since microorganisms have shown capable of withstanding unfavorable conditions for bioremediation [154,209,210], and operate under high pH values and high concentrations of inorganic salts (i.e., $CaCl_2$) [211]. Montmorillonite-coupled MICP in cyanide tailings showed up to a 1.33 increase in precipitation and up to 34.55% CO_2 capture [212]. Other natural environments that supply cations for carbonation include: evaporate deposits, saline aquifers, waste brines, wastes from oil extraction, seawater [213]. MICP has shown success in precipitating carbonate in mine waste [73,154,214–216], concrete and building materials [217–220], coastal and marine environments [38], and agriculture and soil [47,221–223], all of which indirectly demonstrate the promising potential for carbon sequestration utilizing various substrates. Table 4 summarizes research investigating MICP as a method for carbon sequestration.

Table 4. Carbon sequestration using MICP.

Metabolic Pathway	Microbial Strain	Material	Findings	Reference
CA	*Citrobacter freundii*	Wastewater	$CaCO_3$ precipitated with CO_2 catalyzed by CA. Can sequester CO_2 at high concentrations, but HCO_3^- inhibits CA enzyme activity due to pH decrease.	[224]
	Bacillus subtilis	Agar & Liquid Medium	CA converted CO_2 to $CaCO_3$ minerals.	[225]
	Bacillus cereus	Karst Soil	CA enzyme activity influenced $CaCO_3$ crystal morphology.	[226]
	Bacillus megaterium	Mortar Specimens	CO_2 influx precipitated comparable $CaCO_3$ to ureolysis-precipitated $CaCO_3$	[114]

Table 4. *Cont.*

Metabolic Pathway	Microbial Strain	Material	Findings	Reference
	Bacillus pumilus, *Bacillus marisflavi*	Seawater	CA was observed, and precipitates included $CaCO_3 \cdot H_2O$ and $CaCO_3$, showing the potential for carbon sequestration.	[227]
	Bacillus altitudinis	Mangrove Soil	Impact of CO_2 sequestration with bacteria showed 75% removal and 97% removal with bacteria and CA.	[144]
	Bacillus mucilaginosus	Liquid Medium	Optimal CA at 30 °C and alkaline environment to enhance CO_2 hydration.	[228]
	Bacillus mucilaginosus	Liquid Medium	CO_2 is more easily captured by CA, which alters the size and morphology of $CaCO_3$ crystals.	[229]
	Psychrobacter sp., *Vibrio alginolyticus*	Marine Sediments	Strong potential for carbonate precipitation with high CA, meaning capture of CO_2.	[230]
EPS & CA	*Bacillus cereus*	Liquid Medium	Calcite induced by bacteria can fix CO_2 from air since CO_2 released from organic matter is less than in air.	[231]
	Curvibacter lanceolatus	Liquid Medium	CA precipitated only calcite, whereas CA and EPA precipitated calcite and aragonite to enhance CO_2 fixation.	[232]
Phototrophic	*Phragmoplastophyta*	Diamond Mine	Secondary carbonate precipitation capable of offsetting CO_{2e} by 20%.	[129]
	Oscillatoria sp., *Porphyrobacter* sp., *Blastomas* sp., *Rhodobacter* sp.	Diamond Mine	Kimberlite weathering and secondary carbonate precipitation can sequester carbon through photosynthetic bacteria acting as a catalyst to convert CO_2 to $CaCO_3/MgCO_3$.	[130]
Ureolysis	*Sporosarcina*, *Sphingobacterium*, *Stenotrophomonas*, *Acinetobacter*, *Elizabethkingia*	Cave & Tavern Water	CO_2 sequestration depended on pH and the consortia of bacteria.	[113]
	Sporosarcina, *Brevudimonas*, *Sphingobacterium*, *Stenotrophomonas*, *Acinetobacter*	Cave & Tavern Water	Abiotic CO_2 sequestration depended on pH and medium, whereas biotic CO_2 sequestration depended on the bacterial species or strains.	[33]
	Sporosarcina pasteurii	Tailings	MICP increased CO_2 capture from tailings by 27.15–34.55%	[212]

In addition to trapping CO_2 as mineral precipitates, there exists addition mechanisms in which CO_2 can be trapped and therefore stored. MCP and MICP have been utilized to aid CCS methods. During deep geologic injection the CO_2 remains in supercritical state resulting in a distinct phases separate from formation water or brine, which is less dense and viscous permitting CO_2 leakage [162]. Ureolysis and biofilm formation have been used to enhance mineral trapping, solubility trapping, and formation trapping of supercritical CO_2 for geologic carbon sequestration [46,53,153,162,233]. Mineral trapping by precipitation of stable carbonates in deep geologic structures can store carbon but also reduce structural permeability to mitigate CO_2 leakage [234]. Transition-state calcite and siderite have formed in deep saline aquifers by indigenous microorganisms [153]. The formation of biofilms in high-pressure pore spaces can decrease permeability by >95% trapping gaseous CO_2 [46]. Furthermore, a pH increase generated by urea hydrolysis can increase DIC thereby lowering CO_2 gas in the headspace for solubility trapping [233].

While carbonate precipitation can directly trap and store atmospheric CO_2, it can also reduce GHG emissions released to the atmosphere. The cement industry is notorious for its significant contribution to the release of GHG emissions, accounting for 7% of the global GHG emissions and 1.5% (11.2 Mt in 2019) of Canadian emissions [235]. The production of cement (Figure 8) includes mineral extraction of raw materials, mineral processing, raw meal production, clinker formation, cement production and transport [236]. The process produces significant GHG emissions by: (i) calcination reactions (i.e., clinker process; Equation (28)); (ii) combustion of carbon heavy materials (i.e., coal, fuel, natural gas, petroleum coke, etc.); (iii) high energy requirement (2% global energy consumption); (iv) scale of production; (v) material treatment (grinding, mixing, additives); (vi) transport [237]. Self-healing bioconcrete, for example, uses autogenic (chemical reaction precipitating $CaCO_3$ from cement hydration) and autonomic processes (application of encapsulation or a continuous vascular system to distribute a healing agent to precipitate $CaCO_3$; can include MICP) as advancements to concrete repair [219,220]. MCP and MICP can be used as an alternative method for soil and concrete strengthening and restoration of calcareous stones and construction materials [45], reducing the usage of heavy GHG-producing cements. By precipitating $CaCO_3$ or other MCO_3 compounds in the pore space, cracks or fissures, MCP and MICP creates a clogging effect which strengthens the material and reduces compressibility [223]. This is in conjunction with the formation of a biocement matrix, whereby "preferential" and "uniform" distribution of precipitates at particle-particle contacts and precipitation around solid particles respectively, which improves engineering properties [223]. Application of MICP in cementitious materials for the construction industry showed a decrease in CO_2 (3800 ppm to 820 ppm) with precipitated calcite and vaterite crystals through recombinantly produced CA MICP [225]. This shows MICP ability for carbon sequestration and carbon negative cementitious materials [225].

$$CaCO_3 \rightarrow CaO + CO_2 \tag{28}$$

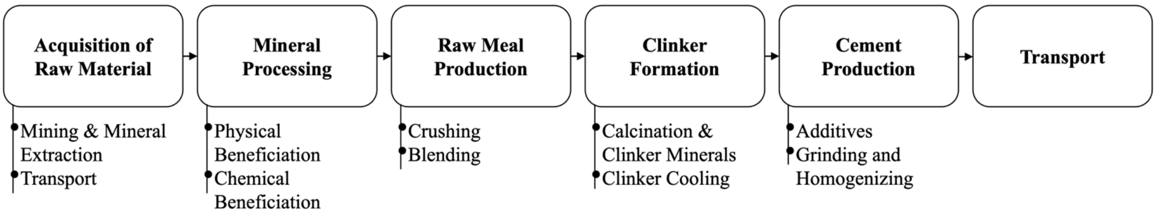

Figure 8. Cement production and the GHG emissions associated with specific processes. Adapted from [236,237].

Finally, MCP and MICP can treat environmental disasters caused by climate change. Increased drought and more severe storms are widely accepted effects of climate change. Earthquake-induced liquefaction causes soil to behave fluidlike because of increases in pore water pressure and decreases in effective stress [238]. MICP has shown promising for treatment of liquefiable saturated soils in-situ [239]. MICP can also be used to treat landslide disasters by strengthening sliding surfaces [240]. Furthermore, both deep flooding and heat stress in soil reduced the relative abundance of genes encoding lignin-degrading catalase in *Actinobacteria*, which resulted in increased organic carbon sequestration [241]. Conversely, drought caused by severe water loss via evaporation can be mitigated with MICP through the formation of a surface crust, remediation of desiccation cracks, smaller pore size, and residual solutes, which decrease the rate of evaporation and water loss by reducing water flow through the material [242].

4. Future Research

While the topic of bacterial carbonatation is not novel, limited research exists on the use of MICP for carbon sequestration. The following is required to better understand microbial carbon sequestration and its long-term feasibility as a CCS technique for the changing environment:

i. Comparisons of MICP utilizing alternative bacteria species to induce different metabolic pathways for the assessment of optimal carbon sequestration.
ii. Suitability of specific bacterial species for use with different material types to establish conducive environmental conditions for their metabolic pathways and activity. To date, most MICP research evaluates its usage with soil. However, additional research is required regarding alternative materials that are less hospitable environments for microorganisms to determine the practicality of biochemical carbon sequestration near GHG point-source emissions.
iii. Analysis of biochemical alterations for enhancement and optimal use of enzyme-driven metabolic pathways. In addition to optimal growth conditions for bacteria, which is regularly incorporated into biochemical analyses, an evaluation of chemical additives and their impact on the efficacy of metalloenzymes (i.e., Ni and Zn) with the objective of carbon sequestration.
iv. Evaluation of MICP and CO_2 injection to better understand preferable CO_2 phases (liquid, gas, supercritical state) for biocalcification and pressures microorganisms can withstand to maximize the rate-limiting CO_2 supply for carbonate precipitation, while minimizing damage to bacterial cells, biomass concentration, and the organic matrix.
v. Comprehensive assessment of bacterial carbonation and its impact on precipitate composition, morphology, and stability for long-term storage of inorganic carbon. Impacts at the micro-particle scale and the large-scale feasibility of carbonate precipitation, considering MICP application and its impact on carbonate stability.
vi. Life-cycle assessments of the MICP process comparing different MICP application methods (i.e., in situ biostimulation, ex situ biostimulation, bioaugmentation, amended bioaugmentation) with traditional carbon sequestration techniques to determine quantitively the carbon emissions vs. carbon sequestered from “cradle” to “grave”.
vii. Evaluation of the long-term feasibility of MICP with the changing environment due to climate change. The geophysical and biochemical environmental changes (temperature, groundwater conditions, etc.) attributed to climate change and their impacts on specific bacterial species and community diversity, their metabolic activity, and their ability to precipitate carbonates.

MCP and MICP are promising biochemical advancements to the field of carbon sequestration. Research objectives specific to carbon sequestration and CCS are required to further advance the biocalcification methods. Laboratory-scale experimentation and modeling techniques can provide essential information for the development of optimal conditions to maximize carbonate precipitation and the feasibility of combatting climate change.

5. Conclusions

Mineral carbonation is an effective method to store atmospheric CO_2 as mineral carbonates via mineral trapping. The mechanism is facilitated by numerous biogenic and abiogenic precipitation techniques with varying degrees of microbial control. Enzyme-driven MICP utilizing CA and urease synergistically is promising for catalysis of CO_2 hydration and increase in pH and DIC, leading to increased $CaCO_3$ precipitation. Since increases in $CaCO_3$ precipitation are directly linked to increases in carbon sequestration, optimization of microbial metabolic activity can favorably impact $CaCO_3$ and, therefore, carbon sequestration. Furthermore, solubility trapping and formation trapping via MICP during deep geologic injection of CO_2 can mitigate CO_2 leakage. Biological carbonate precipitation is promising for atmospheric carbon sequestration with the changing climate. Addition experimental research is required to evaluate the reliability of the method.

Author Contributions: Initial draft, S.M.W.; review and revision of the manuscript, C.N.M. and C.M.N. All authors have read and agreed to the published version of the manuscript.

Funding: This research was supported by Concordia University and NSERC (grant Number RGPIN-2021-03471).

Data Availability Statement: Data are contained within the article.

Conflicts of Interest: The authors declare no conflicts of interest.

References

1. Calvin, K.; Dasgupta, D.; Krinner, G.; Mukherji, A.; Thorne, P.W.; Trisos, C.; Romero, J.; Aldunce, P.; Barrett, K.; Blanco, G.; et al. *IPCC, 2023: Climate Change 2023: Synthesis Report. Contribution of Working Groups I, II and III to the Sixth Assessment Report of the Intergovernmental Panel on Climate Change*; Core Writing Team, Lee, H., Romero, J., Eds.; Intergovernmental Panel on Climate Change (IPCC), 2023; IPCC: Geneva, Switzerland, 2023.
2. Gayathri, R.; Mahboob, S.; Govindarajan, M.; Al-Ghanim, K.A.; Ahmed, Z.; Al-Mulhm, N.; Vodovnik, M.; Vijayalakshmi, S. A Review on Biological Carbon Sequestration: A Sustainable Solution for a Cleaner Air Environment, Less Pollution and Lower Health Risks. *J. King Saud Univ. Sci.* **2021**, *33*, 101282. [CrossRef]
3. Oves, M.; Hussain, F.M.; Ismail, I.M.I.; Felemban, N.M.; Qari, H.A. Microbiological Carbon Sequestration: A Novel Solution for Atmospheric Carbon–Carbon Sequestration through Biological Approach. In *Handbook of Research on Inventive Bioremediation Techniques*; IGI Global: Hershey, PA, USA, 2017; pp. 108–133. ISBN 978-1-5225-2325-3.
4. Karpiński, P.H.; Bałdyga, J. Chapter 8—Precipitation Processes. In *Handbook of Industrial Crystallization*; Myerson, A.S., Erdemir, D., Lee, A.Y., Eds.; Cambridge University Press: Cambridge, UK, 2019; pp. 216–265. ISBN 978-1-139-02694-9.
5. Lewis, A. Chapter 4—Precipitation of Heavy Metals. In *Sustainable Heavy Metal Remediation: Volume 1: Principles and Processes*; Rene, E.R., Sahinkaya, E., Lewis, A., Lens, P.N.L., Eds.; Environmental Chemistry for a Sustainable World; Springer International Publishing: Cham, Switzerland, 2017; pp. 101–120. ISBN 978-3-319-58622-9.
6. The Editors of Encyclopaedia Britannica Chemical Precipitation | Britannica. Available online: https://www.britannica.com/science/chemical-precipitation (accessed on 29 March 2023).
7. Wang, L.K.; Vaccari, D.A.; Li, Y.; Shammas, N.K. Chapter 5—Chemical Precipitation. In *Physicochemical Treatment Processes*; Wang, L.K., Hung, Y.-T., Shammas, N.K., Eds.; Handbook of Environmental Engineering; Humana Press: Totowa, NJ, USA, 2005; pp. 141–197. ISBN 978-1-59259-820-5.
8. Yong, R.N.; Mulligan, C.N.; Fukue, M. *Sustainable Practices in Geoenvironmental Engineering*, 2nd ed.; CRC Press: Boca Raton, FL, USA, 2014; ISBN 978-0-429-16839-0.
9. Chakhmouradian, A.R.; Zaitsev, A.N. Rare Earth Mineralization in Igneous Rocks: Sources and Processes. *Elements* **2012**, *8*, 347–353. [CrossRef]
10. Morse, J.W.; Arvidson, R.S. The Dissolution Kinetics of Major Sedimentary Carbonate Minerals. *Earth Sci. Rev.* **2002**, *58*, 51–84. [CrossRef]

11. Wada, H.; Tomita, T.; Matsuura, K.; Tuchi, K.; Ito, M.; Morikiyo, T. Graphitization of Carbonaceous Matter during Metamorphism with References to Carbonate and Pelitic Rocks of Contact and Regional Metamorphisms, Japan. *Contr. Mineral. Petrol.* **1994**, *118*, 217–228. [CrossRef]
12. James, N.P.; Jones, B. *Origin of Carbonate Sedimentary Rocks*; John Wiley & Sons: Hoboken, NJ, USA, 2015; ISBN 978-1-118-65270-1.
13. Gregg, J.M.; Bish, D.L.; Kaczmarek, S.E.; Machel, H.G. Mineralogy, Nucleation and Growth of Dolomite in the Laboratory and Sedimentary Environment: A Review. *Sedimentology* **2015**, *62*, 1749–1769. [CrossRef]
14. Zhang, G.; Morales, J.; Manuel García-Ruiz, J. Growth Behaviour of Silica/Carbonate Nanocrystalline Composites of Calcite and Aragonite. *J. Mater. Chem. B* **2017**, *5*, 1658–1663. [CrossRef]
15. Gonzalez, L.A.; Carpenter, S.J.; Lohmann, K.C. Inorganic Calcite Morphology; Roles of Fluid Chemistry and Fluid Flow. *J. Sediment. Res.* **1992**, *62*, 382–399. [CrossRef]
16. Folk, R.L. The Natural History of Crystalline Calcium Carbonate; Effect of Magnesium Content and Salinity. *J. Sediment. Res.* **1974**, *44*, 40–53. [CrossRef]
17. Lahann, R.W. A Chemical Model for Calcite Crystal Growth and Morphology Control. *J. Sediment. Res.* **1978**, *48*, 337–347. [CrossRef]
18. Zhang, Y.; Dawe, R.A. Influence of Mg2+ on the Kinetics of Calcite Precipitation and Calcite Crystal Morphology. *Chem. Geol.* **2000**, *163*, 129–138. [CrossRef]
19. Weyl, P.K. The Change in Solubility of Calcium Carbonate with Temperature and Carbon Dioxide Content. *Geochim. Cosmochim. Acta* **1959**, *17*, 214–225. [CrossRef]
20. Brečević, L.; Nielsen, A.E. Solubility of Amorphous Calcium Carbonate. *J. Cryst. Growth* **1989**, *98*, 504–510. [CrossRef]
21. Harvey, O.R.; Qafoku, N.P.; Cantrell, K.J.; Lee, G.; Amonette, J.E.; Brown, C.F. Geochemical Implications of Gas Leakage Associated with Geologic CO_2 Storage—A Qualitative Review. *Environ. Sci. Technol.* **2013**, *47*, 23–36. [CrossRef] [PubMed]
22. Taft, W. Modern Carbonate Sediments. In *Carbonate Rocks: Origin, Occurence and Classification*; Chilingar, G.V., Bissell, H.J., Fairbridge, R.W., Eds.; Developments in Sedimentology; Elsevier Pub. Co.: Amsterdam, The Netherlands, 1967.
23. Wu, S. Classification of Biogenic Carbonate Rocks. *Biopetrology* **2021**, *1*, 19–29.
24. Chilingar, G.V.; Bissell, H.J.; Wolf, K.H. Chapter 5 Diagenesis of Carbonate Rocks. In *Developments in Sedimentology*; Larsen, G., Chilingar, G.V., Eds.; Diagenesis in Sediments; Elsevier: Amsterdam, The Netherlands, 1967; Volume 8, pp. 179–322.
25. Fairbridge, R.W.; Chilingar, G.V.; Bissell, H.J. Introduction. In *Carbonate Rocks: Origin, Occurence and Classification*; Chilingarian, G.V., Bissell, H.J., Fairbridge, R.W., Eds.; Developments in Sedimentology; Elsevier Pub. Co.: Amsterdam, The Netherlands, 1967.
26. Castro-Alonso, M.J.; Montañez-Hernandez, L.E.; Sanchez-Muñoz, M.A.; Macias Franco, M.R.; Narayanasamy, R.; Balagurusamy, N. Microbially Induced Calcium Carbonate Precipitation (MICP) and Its Potential in Bioconcrete: Microbiological and Molecular Concepts. *Front. Mater.* **2019**, *6*, 126. [CrossRef]
27. Joshi, S.; Goyal, S.; Sudhakara Reddy, M. Influence of Biogenic Treatment in Improving the Durability Properties of Waste Amended Concrete: A Review. *Constr. Build. Mater.* **2020**, *263*, 120170. [CrossRef]
28. Kumar, R.; Nongkhlaw, M.; Acharya, C.; Joshi, S.R. Bacterial Community Structure from the Perspective of the Uranium Ore Deposits of Domiasiat in India. *Proc. Natl. Acad. Sci. India Sect. B Biol. Sci.* **2013**, *83*, 485–497. [CrossRef]
29. Weiner, S.; Dove, P.M. An Overview of Biomineralization Processes and the Problem of the Vital Effect. *Rev. Mineral. Geochem.* **2003**, *54*, 1–29. [CrossRef]
30. Zhuang, D.; Yan, H.; Tucker, M.E.; Zhao, H.; Han, Z.; Zhao, Y.; Sun, B.; Li, D.; Pan, J.; Zhao, Y.; et al. Calcite Precipitation Induced by *Bacillus Cereus* MRR2 Cultured at Different Ca^{2+} Concentrations: Further Insights into Biotic and Abiotic Calcite. *Chem. Geol.* **2018**, *500*, 64–87. [CrossRef]
31. Kelts, K.; Talbot, M. Lacustrine Carbonates as Geochemical Archives of Environmental Change and Biotic/Abiotic Interactions. In *Large Lakes: Ecological Structure and Function*; Tilzer, M.M., Serruya, C., Eds.; Springer: Berlin/Heidelberg, Germany, 1990; pp. 288–315. ISBN 978-3-642-84077-7.
32. Rainey, D.K.; Jones, B. Abiotic versus Biotic Controls on the Development of the Fairmont Hot Springs Carbonate Deposit, British Columbia, Canada. *Sedimentology* **2009**, *56*, 1832–1857. [CrossRef]
33. Okyay, T.O.; Rodrigues, D.F. Biotic and Abiotic Effects on CO_2 Sequestration during Microbially-Induced Calcium Carbonate Precipitation. *FEMS Microbiol. Ecol.* **2015**, *91*, fiv017. [CrossRef] [PubMed]
34. Anbu, P.; Kang, C.-H.; Shin, Y.-J.; So, J.-S. Formations of Calcium Carbonate Minerals by Bacteria and Its Multiple Applications. *Springerplus* **2016**, *5*, 250. [CrossRef] [PubMed]
35. Mujah, D.; Shahin, M.; Cheng, L. State-of-the-Art Review of Biocementation by Microbially Induced Calcite Precipitation (MICP) for Soil Stabilization. *Geomicrobiology* **2016**, *34*, 524–537. [CrossRef]
36. Dhami, N.K.; Reddy, M.S.; Mukherjee, A. Biomineralization of Calcium Carbonates and Their Engineered Applications: A Review. *Front. Microbiol.* **2013**, *4*, 314. [CrossRef]
37. Benzerara, K.; Miot, J.; Morin, G.; Ona-Nguema, G.; Skouri-Panet, F.; Férard, C. Significance, Mechanisms and Environmental Implications of Microbial Biomineralization. *Comptes Rendus Geosci.* **2011**, *343*, 160–167. [CrossRef]

38. Dupraz, C.; Reid, R.P.; Braissant, O.; Decho, A.W.; Norman, R.S.; Visscher, P.T. Processes of Carbonate Precipitation in Modern Microbial Mats. *Earth Sci. Rev.* **2009**, *96*, 141–162. [CrossRef]
39. De Deyn, G.B.; Cornelissen, J.H.C.; Bardgett, R.D. Plant Functional Traits and Soil Carbon Sequestration in Contrasting Biomes. *Ecol. Lett.* **2008**, *11*, 516–531. [CrossRef]
40. Lal, R. Carbon Sequestration. *Philos. Trans. R. Soc. B Biol. Sci.* **2007**, *363*, 815–830. [CrossRef]
41. Farrelly, D.J.; Everard, C.D.; Fagan, C.C.; McDonnell, K.P. Carbon Sequestration and the Role of Biological Carbon Mitigation: A Review. *Renew. Sustain. Energy Rev.* **2013**, *21*, 712–727. [CrossRef]
42. Liu, D.-X.; Mai, Z.-M.; Sun, C.-C.; Zhou, Y.-W.; Liao, H.-H.; Wang, Y.-S.; Cheng, H. Dynamics of Extracellular Polymeric Substances and Soil Organic Carbon with Mangrove Zonation along a Continuous Tidal Gradient. *Front. Mar. Sci.* **2022**, *9*, 967767. [CrossRef]
43. Alongi, D.M. Carbon Cycling and Storage in Mangrove Forests. *Annu. Rev. Mar. Sci.* **2014**, *6*, 195–219. [CrossRef] [PubMed]
44. Konhauser, K. *Introduction to Geomicrobiology*; Blackwell Publishing: Oxford, UK, 2007; ISBN 978-0-632-05454-1.
45. Wilcox, S.M.; Mulligan, C.N.; Neculita, C.M. Microbially Induced Calcium Carbonate Precipitation as a Bioremediation Technique for Mining Waste. *Toxics* **2024**, *12*, 107. [CrossRef] [PubMed]
46. Mitchell, A.C.; Phillips, A.J.; Hiebert, R.; Gerlach, R.; Spangler, L.H.; Cunningham, A.B. Biofilm Enhanced Geologic Sequestration of Supercritical CO_2. *Int. J. Greenh. Gas Control* **2009**, *3*, 90–99. [CrossRef]
47. Jiang, N.-J.; Wang, Y.-J.; Chu, J.; Kawasaki, S.; Tang, C.-S.; Cheng, L.; Du, Y.-J.; Shashank, B.S.; Singh, D.N.; Han, X.-L.; et al. Bio-Mediated Soil Improvement: An Introspection into Processes, Materials, Characterization and Applications. *Soil Use Manag.* **2022**, *38*, 68–93. [CrossRef]
48. Madigan, M.T.; Bender, K.S.; Buckley, D.H.; Sattley, W.M.; Stahl, D.A. *Brock Biology of Microorganisms*, 15th ed.; Global Edition; Pearson: New York, NY, USA, 2019; ISBN 978-1-292-23510-3.
49. Westbroek, P.; Brown, C.W.; van Bleijswijk, J.; Brownlee, C.; Brummer, G.J.; Conte, M.; Egge, J.; Fernández, E.; Jordan, R.; Knappertsbusch, M.; et al. A Model System Approach to Biological Climate Forcing. The Example of Emiliania Huxleyi. *Glob. Planet. Change* **1993**, *8*, 27–46. [CrossRef]
50. Riebesell, U.; Zondervan, I.; Rost, B.; Tortell, P.D.; Zeebe, R.E.; Morel, F.M.M. Reduced Calcification of Marine Plankton in Response to Increased Atmospheric CO_2. *Nature* **2000**, *407*, 364–367. [CrossRef]
51. Berg, I.A.; Kockelkorn, D.; Ramos-Vera, W.H.; Say, R.F.; Zarzycki, J.; Hügler, M.; Alber, B.E.; Fuchs, G. Autotrophic Carbon Fixation in Archaea. *Nat. Rev. Microbiol* **2010**, *8*, 447–460. [CrossRef]
52. Hammes, F.; Verstraete, W. Key Roles of pH and Calcium Metabolism in Microbial Carbonate Precipitation. *Rev. Environ. Sci. Biotechnol.* **2002**, *1*, 3–7. [CrossRef]
53. Phillips, A.J.; Gerlach, R.; Lauchnor, E.; Mitchell, A.C.; Cunningham, A.B.; Spangler, L. Engineered Applications of Ureolytic Biomineralization: A Review. *Biofouling* **2013**, *29*, 715–733. [CrossRef]
54. Achal, V.; Pan, X. Characterization of Urease and Carbonic Anhydrase Producing Bacteria and Their Role in Calcite Precipitation. *Curr. Microbiol.* **2011**, *62*, 894–902. [CrossRef]
55. Douglas, S.; Beveridge, T.J. Mineral Formation by Bacteria in Natural Microbial Communities. *FEMS Microbiol. Ecol.* **1998**, *26*, 79–88. [CrossRef]
56. Kapahi, M.; Sachdeva, S. Bioremediation Options for Heavy Metal Pollution. *J. Health Pollut.* **2019**, *9*, 191203. [CrossRef] [PubMed]
57. Yee, N.; Fein, J.B.; Daughney, C.J. Experimental Study of the pH, Ionic Strength, and Reversibility Behavior of Bacteria–Mineral Adsorption. *Geochim. Cosmochim. Acta* **2000**, *64*, 609–617. [CrossRef]
58. Zhu, T.; Dittrich, M. Carbonate Precipitation through Microbial Activities in Natural Environment, and Their Potential in Biotechnology: A Review. *Front. Bioeng. Biotechnol.* **2016**, *4*, 4. [CrossRef]
59. Xiangliang, P. Micrologically Induced Carbonate Precipitation as a Promising Way to in Situ Immobilize Heavy Metals in Groundwater and Sediment. *Res. J. Chem. Environ.* **2009**, *13*, 3–4.
60. Achal, V.; Mukherjee, A.; Basu, P.C.; Reddy, M.S. Strain Improvement of *Sporosarcina pasteurii* for Enhanced Urease and Calcite Production. *J. Ind. Microbiol. Biotechnol.* **2009**, *36*, 981–988. [CrossRef]
61. Ferris, F.G.; Fyfe, W.S.; Beveridge, T.J. Bacteria as Nucleation Sites for Authigenic Minerals in a Metal-Contaminated Lake Sediment. *Chem. Geol.* **1987**, *63*, 225–232. [CrossRef]
62. Costa, O.Y.A.; Raaijmakers, J.M.; Kuramae, E.E. Microbial Extracellular Polymeric Substances: Ecological Function and Impact on Soil Aggregation. *Front. Microbiol.* **2018**, *9*, 1636. [CrossRef]
63. Dittrich, M.; Sibler, S. Calcium Carbonate Precipitation by Cyanobacterial Polysaccharides. *Geol. Soc. Lond. Spec. Publ.* **2010**, *336*, 51–63. [CrossRef]
64. Tourney, J.; Ngwenya, B.T.; Mosselmans, J.W.F.; Tetley, L.; Cowie, G.L. The Effect of Extracellular Polymers (EPS) on the Proton Adsorption Characteristics of the Thermophile Bacillus Licheniformis S-86. *Chem. Geol.* **2008**, *247*, 1–15. [CrossRef]
65. Kawaguchi, T.; Decho, A.W. A Laboratory Investigation of Cyanobacterial Extracellular Polymeric Secretions (EPS) in Influencing $CaCO_3$ Polymorphism. *J. Cryst. Growth* **2002**, *240*, 230–235. [CrossRef]

66. Kim, J.-H.; Lee, J.-Y. An Optimum Condition of MICP Indigenous Bacteria with Contaminated Wastes of Heavy Metal. *J. Mater. Cycles Waste Manag.* **2019**, *21*, 239–247. [CrossRef]
67. Tourney, J.; Ngwenya, B.T. Bacterial Extracellular Polymeric Substances (EPS) Mediate $CaCO_3$ Morphology and Polymorphism. *Chem. Geol.* **2009**, *262*, 138–146. [CrossRef]
68. Dejong, J.t.; Soga, K.; Kavazanjian, E.; Burns, S.; Van Paassen, L.a.; Al Qabany, A.; Aydilek, A.; Bang, S.s.; Burbank, M.; Caslake, L.f.; et al. Biogeochemical Processes and Geotechnical Applications: Progress, Opportunities and Challenges. *Géotechnique* **2013**, *63*, 287–301. [CrossRef]
69. Achal, V.; Li, M.; Zhang, Q. Biocement, Recent Research in Construction Engineering: Status of China against Rest of World. *Adv. Cem. Res.* **2014**, *26*, 281–291. [CrossRef]
70. Fenchel, T.; King, G.M.; Blackburn, T.H. *Bacterial Biogeochemistry: The Ecophysiology of Mineral Cycling*; Academic Press: Cambridge, MA, USA, 2012; ISBN 978-0-12-415836-8.
71. Fontaine, S.; Mariotti, A.; Abbadie, L. The Priming Effect of Organic Matter: A Question of Microbial Competition? *Soil Biol. Biochem.* **2003**, *35*, 837–843. [CrossRef]
72. Pepper, I.L.; Gerba, C.P.; Gentry, T.J. *Environmental Microbiology*, 3rd ed.; Elsevier: Amsterdam, The Netherlands, 2015; ISBN 978-0-12-394626-3.
73. Govarthanan, M.; Lee, K.-J.; Cho, M.; Kim, J.S.; Kamala-Kannan, S.; Oh, B.-T. Significance of *Autochthonous bacillus* sp. KK1 on Biomineralization of Lead in Mine Tailings. *Chemosphere* **2013**, *90*, 2267–2272. [CrossRef]
74. Bang, S. Microbiologically-Enhanced Crack Remediation (MECR). *Proc. Microbiol. Soc. Korea Conf.* **2001**, *11*, 26–36.
75. Chuo, S.C.; Mohamed, S.F.; Mohd Setapar, S.H.; Ahmad, A.; Jawaid, M.; Wani, W.A.; Yaqoob, A.A.; Mohamad Ibrahim, M.N. Insights into the Current Trends in the Utilization of Bacteria for Microbially Induced Calcium Carbonate Precipitation. *Materials* **2020**, *13*, 4993. [CrossRef]
76. Graddy, C.M.R.; Gomez, M.G.; DeJong, J.T.; Nelson, D.C. Native Bacterial Community Convergence in Augmented and Stimulated Ureolytic MICP Biocementation. *Environ. Sci. Technol.* **2021**, *55*, 10784–10793. [CrossRef]
77. McConnaughey, T.A.; Whelan, J.F. Calcification Generates Protons for Nutrient and Bicarbonate Uptake. *Earth Sci. Rev.* **1997**, *42*, 95–117. [CrossRef]
78. Castanier, S.; Le Métayer-Levrel, G.; Perthuisot, J.-P. Ca-Carbonates Precipitation and Limestone Genesis—The Microbiogeologist Point of View. *Sediment. Geol.* **1999**, *126*, 9–23. [CrossRef]
79. Norris, V.; Grant, S.; Freestone, P.; Canvin, J.; Sheikh, F.N.; Toth, I.; Trinei, M.; Modha, K.; Norman, R.I. Calcium Signalling in Bacteria. *J. Bacteriol.* **1996**, *178*, 3677–3682. [CrossRef]
80. Kumar, A.; Song, H.-W.; Mishra, S.; Zhang, W.; Zhang, Y.-L.; Zhang, Q.-R.; Yu, Z.-G. Application of Microbial-Induced Carbonate Precipitation (MICP) Techniques to Remove Heavy Metal in the Natural Environment: A Critical Review. *Chemosphere* **2023**, *318*, 137894. [CrossRef]
81. Rahman, M.M.; Hora, R.N.; Ahenkorah, I.; Beecham, S.; Karim, M.R.; Iqbal, A. State-of-the-Art Review of Microbial-Induced Calcite Precipitation and Its Sustainability in Engineering Applications. *Sustainability* **2020**, *12*, 6281. [CrossRef]
82. Olaya-Abril, A.; Hidalgo-Carrillo, J.; Luque-Almagro, V.M.; Fuentes-Almagro, C.; Urbano, F.J.; Moreno-Vivián, C.; Richardson, D.J.; Roldán, M.D. Exploring the Denitrification Proteome of Paracoccus Denitrificans PD1222. *Front. Microbiol.* **2018**, *9*, 1137. [CrossRef]
83. van Paassen, L.A.; Daza, C.M.; Staal, M.; Sorokin, D.Y.; van der Zon, W.; van Loosdrecht, M.C.M. Potential Soil Reinforcement by Biological Denitrification. *Ecol. Eng.* **2010**, *36*, 168–175. [CrossRef]
84. Hamdan, N.; Kavazanjian, E.; Rittmann, B.E.; Karatas, I. Carbonate Mineral Precipitation for Soil Improvement through Microbial Denitrification. *Geomicrobiol. J.* **2017**, *34*, 139–146. [CrossRef]
85. Liang, Y.; Fu, R.; Sailike, A.; Hao, H.; Yu, Z.; Wang, R.; Peng, N.; Li, S.; Zhang, W.; Liu, Y. Soil Labile Organic Carbon and Nitrate Nitrogen Are the Main Factors Driving Carbon-Fixing Pathways during Vegetation Restoration in the Loess Plateau, China. *Agric. Ecosyst. Environ.* **2025**, *378*, 109283. [CrossRef]
86. Ren, M.; Zhang, Z.; Wang, X.; Zhou, Z.; Chen, D.; Zeng, H.; Zhao, S.; Chen, L.; Hu, Y.; Zhang, C.; et al. Diversity and Contributions to Nitrogen Cycling and Carbon Fixation of Soil Salinity Shaped Microbial Communities in Tarim Basin. *Front. Microbiol.* **2018**, *9*, 431. [CrossRef]
87. Chekroun, K.B.; Rodríguez-Navarro, C.; González-Muñoz, M.T.; Arias, J.M.; Cultrone, G.; Rodríguez-Gallego, M. Precipitation and Growth Morphology of Calcium Carbonate Induced by *Myxococcus xanthus*: Implications for Recognition of Bacterial Carbonates. *J. Sediment. Res.* **2004**, *74*, 868–876. [CrossRef]
88. Jiménez-López, C.; Jroundi, F.; Rodríguez-Gallego, M.; Arias, J.; Gonzalez, M.T. Biomineralization Induced by Myxobacteria. In *Communicating Current Research and Educational Topics and Trends in Applied Microbiology*; Méndez-Vilas, A., Ed.; Formatex Research Center: Oviedo, Spain, 2007.

89. Marín-Ortega, S.; Torras, M.À.C.i.; Iglesias-Campos, M.Á. Microbially Induced Calcium Carbonate Precipitation in Fossil Consolidation Treatments: Preliminary Results Inducing Exogenous *Myxococcus xanthus* Bacteria in a Miocene Cheirogaster Richardi Specimen. *Heliyon* **2023**, *9*, e17597. [CrossRef] [PubMed]
90. Keena, M.; Meehan, M.; Scherer, T. *Nitrogen Behaviour in the Environment*; North Dakota State University: Fargo, ND, USA, 2022.
91. Lee, M.; Gomez, M.G.; San Pablo, A.C.M.; Kolbus, C.M.; Graddy, C.M.R.; DeJong, J.T.; Nelson, D.C. Investigating Ammonium by-Product Removal for Ureolytic Bio-Cementation Using Meter-Scale Experiments. *Sci. Rep.* **2019**, *9*, 18313. [CrossRef] [PubMed]
92. Joshi, S.; Goyal, S.; Mukherjee, A.; Reddy, M.S. Microbial Healing of Cracks in Concrete: A Review. *J. Ind. Microbiol. Biotechnol.* **2017**, *44*, 1511–1525. [CrossRef]
93. Dhami, N.K.; Reddy, M.S.; Mukherjee, A. Synergistic Role of Bacterial Urease and Carbonic Anhydrase in Carbonate Mineralization. *Appl. Biochem. Biotechnol.* **2014**, *172*, 2552–2561. [CrossRef]
94. Stocks-Fischer, S.; Galinat, J.K.; Bang, S.S. Microbiological Precipitation of $CaCO_3$. *Soil Biol. Biochem.* **1999**, *31*, 1563–1571. [CrossRef]
95. Hasan, H.A.H. Ureolytic Microorganisms and Soil Fertility: A Review. *Commun. Soil Sci. Plant Anal.* **2000**, *31*, 2565–2589. [CrossRef]
96. Zerner, B. Recent Advances in the Chemistry of an Old Enzyme, Urease. *Bioorganic Chem.* **1991**, *19*, 116–131. [CrossRef]
97. Callahan, B.P.; Yuan, Y.; Wolfenden, R. The Burden Borne by Urease. *J. Am. Chem. Soc.* **2005**, *127*, 10828–10829. [CrossRef]
98. Ciurli, S. Urease: Recent Insights on the Role of Nickel. In *Nickel and Its Surprising Impact in Nature*; John Wiley & Sons, Ltd.: Hoboken, NJ, USA, 2007; pp. 241–277. ISBN 978-0-470-02813-1.
99. Su, F.; Yang, Y.Y. Microbially Induced Carbonate Precipitation via Methanogenesis Pathway by a Microbial Consortium Enriched from Activated Anaerobic Sludge. *J. Appl. Microbiol.* **2021**, *131*, 236–256. [CrossRef]
100. DeJong, J.; Proto, C.; Kuo, M.; Gomez, M. Bacteria, Biofilms, and Invertebrates: The next Generation of Geotechnical Engineers? In Proceedings of the Geo-Congress 2014, Atlanta, GA, USA, 23–26 February 2014; pp. 3959–3968. [CrossRef]
101. Buikema, N.D.; Zwissler, B.E.; Seagren, E.A.; Oommen, T.; Vitton, S. Stabilisation of Iron Mine Tailings through Biocalcification. *Environ. Geotech.* **2018**, *5*, 94–106. [CrossRef]
102. Stabnikov, V.; Ivanov, V. Biotechnological Production of Biogrout from Iron Ore and Cellulose. *J. Chem. Technol. Biotechnol.* **2017**, *92*, 180–187. [CrossRef]
103. Yao, Y.; Wang, L.; Hemamali Peduruhewa, J.; Van Zwieten, L.; Gong, L.; Tan, B.; Zhang, G. The Coupling between Iron and Carbon and Iron Reducing Bacteria Control Carbon Sequestration in Paddy Soils. *CATENA* **2023**, *223*, 106937. [CrossRef]
104. Chen, C.; Dynes, J.J.; Wang, J.; Sparks, D.L. Properties of Fe-Organic Matter Associations via Coprecipitation versus Adsorption. *Environ. Sci. Technol.* **2014**, *48*, 13751–13759. [CrossRef] [PubMed]
105. Lalonde, K.; Mucci, A.; Ouellet, A.; Gélinas, Y. Preservation of Organic Matter in Sediments Promoted by Iron. *Nature* **2012**, *483*, 198–200. [CrossRef]
106. Bergdale, T.E.; Pinkelman, R.J.; Hughes, S.R.; Zambelli, B.; Ciurli, S.; Bang, S.S. Engineered Biosealant Strains Producing Inorganic and Organic Biopolymers. *J. Biotechnol.* **2012**, *161*, 181–189. [CrossRef]
107. Zambelli, B.; Musiani, F.; Benini, S.; Ciurli, S. Chemistry of Ni2+ in Urease: Sensing, Trafficking, and Catalysis. *Acc. Chem. Res.* **2011**, *44*, 520–530. [CrossRef]
108. Svane, S.; Sigurdarson, J.J.; Finkenwirth, F.; Eitinger, T.; Karring, H. Inhibition of Urease Activity by Different Compounds Provides Insight into the Modulation and Association of Bacterial Nickel Import and Ureolysis. *Sci. Rep.* **2020**, *10*, 8503. [CrossRef]
109. Lv, J.; Jiang, Y.; Yu, Q.; Lu, S. Structural and Functional Role of Nickel Ions in Urease by Molecular Dynamics Simulation. *J. Biol. Inorg. Chem.* **2011**, *16*, 125–135. [CrossRef]
110. Estiu, G.; Merz, K.M. Catalyzed Decomposition of Urea. Molecular Dynamics Simulations of the Binding of Urea to Urease. *Biochemistry* **2006**, *45*, 4429–4443. [CrossRef]
111. Bachmeier, K.L.; Williams, A.E.; Warmington, J.R.; Bang, S.S. Urease Activity in Microbiologically-Induced Calcite Precipitation. *J. Biotechnol.* **2002**, *93*, 171–181. [CrossRef] [PubMed]
112. Okyay, T.O.; Rodrigues, D.F. Optimized Carbonate Micro-Particle Production by *Sporosarcina pasteurii* Using Response Surface Methodology. *Ecol. Eng.* **2014**, *62*, 168–174. [CrossRef]
113. Okyay, T.O.; Nguyen, H.N.; Castro, S.L.; Rodrigues, D.F. CO_2 Sequestration by Ureolytic Microbial Consortia through Microbially-Induced Calcite Precipitation. *Sci. Total Environ.* **2016**, *572*, 671–680. [CrossRef]
114. Kaur, G.; Dhami, N.K.; Goyal, S.; Mukherjee, A.; Reddy, M.S. Utilization of Carbon Dioxide as an Alternative to Urea in Biocementation. *Constr. Build. Mater.* **2016**, *123*, 527–533. [CrossRef]
115. Sánchez-Andrea, I.; Sanz, J.L.; Bijmans, M.F.M.; Stams, A.J.M. Sulfate Reduction at Low pH to Remediate Acid Mine Drainage. *J. Hazard. Mater.* **2014**, *269*, 98–109. [CrossRef]
116. Sánchez-Andrea, I.; Stams, A.J.M.; Weijma, J.; Gonzalez Contreras, P.; Dijkman, H.; Rozendal, R.A.; Johnson, D.B. A Case in Support of Implementing Innovative Bio-Processes in the Metal Mining Industry. *FEMS Microbiol. Lett.* **2016**, *363*, 1–4. [CrossRef]

117. Paul, V.G.; Wronkiewicz, D.J.; Mormile, M.R. Impact of Elevated CO_2 Concentrations on Carbonate Mineral Precipitation Ability of Sulfate-Reducing Bacteria and Implications for CO_2 Sequestration. *Appl. Geochem.* **2017**, *78*, 250–271. [CrossRef]
118. Pester, M.; Knorr, K.-H.; Friedrich, M.W.; Wagner, M.; Loy, A. Sulfate-Reducing Microorganisms in Wetlands—Fameless Actors in Carbon Cycling and Climate Change. *Front. Microbiol.* **2012**, *3*, 19769. [CrossRef]
119. Visscher, P.T.; Reid, R.P.; Bebout, B.M.; Hoeft, S.E.; Macintyre, I.G.; Thompson, J.A. Formation of Lithified Micritic Laminae in Modern Marine Stromatolites (Bahamas); The Role of Sulfur Cycling. *Am. Mineral.* **1998**, *83*, 1482–1493. [CrossRef]
120. Görgen, S.; Benzerara, K.; Skouri-Panet, F.; Gugger, M.; Chauvat, F.; Cassier-Chauvat, C. The Diversity of Molecular Mechanisms of Carbonate Biomineralization by Bacteria. *Discov. Mater.* **2020**, *1*, 2. [CrossRef]
121. Akam, S.A.; Swanner, E.D.; Yao, H.; Hong, W.-L.; Peckmann, J. Methane-Derived Authigenic Carbonates—A Case for a Globally Relevant Marine Carbonate Factory. *Earth Sci. Rev.* **2023**, *243*, 104487. [CrossRef]
122. Caesar, K.H.; Kyle, J.R.; Lyons, T.W.; Tripati, A.; Loyd, S.J. Carbonate Formation in Salt Dome Cap Rocks by Microbial Anaerobic Oxidation of Methane. *Nat. Commun.* **2019**, *10*, 808. [CrossRef] [PubMed]
123. Jain, S.; Fang, C.; Achal, V. A Critical Review on Microbial Carbonate Precipitation via Denitrification Process in Building Materials. *Bioengineered* **2021**, *12*, 7529–7551. [CrossRef] [PubMed]
124. Rasigraf, O.; Kool, D.M.; Jetten, M.S.M.; Sinninghe Damsté, J.S.; Ettwig, K.F. Autotrophic Carbon Dioxide Fixation via the Calvin-Benson-Bassham Cycle by the Denitrifying Methanotroph "*Candidatus* Methylomirabilis Oxyfera". *Appl. Environ. Microbiol.* **2014**, *80*, 2451–2460. [CrossRef]
125. Smith, K.S.; Ferry, J.G. Prokaryotic Carbonic Anhydrases. *FEMS Microbiol. Rev.* **2000**, *24*, 335–366. [CrossRef]
126. Altermann, W.; Kazmierczak, J.; Oren, A.; Wright, D.T. Cyanobacterial Calcification and Its Rock-Building Potential during 3.5 Billion Years of Earth History. *Geobiology* **2006**, *4*, 147–166. [CrossRef]
127. Verrecchia, E.P.; Freytet, P.; Verrecchia, K.E.; Dumont, J.-L. Spherulites in Calcrete Laminar Crusts; Biogenic CaCO 3 Precipitation as a Major Contributor to Crust Formation. *J. Sediment. Res.* **1995**, *65*, 690–700. [CrossRef]
128. Pentecost, A. The Formation of Travertine Shrubs: Mammoth Hot Springs, Wyoming. *Geol. Mag.* **1990**, *127*, 159–168. [CrossRef]
129. Jones, T.R.; Poitras, J.; Levett, A.; Langendam, A.; Vietti, A.; Southam, G. Accelerated Carbonate Biomineralisation of Venetia Diamond Mine Coarse Residue Deposit (CRD) Material—A Field Trial Study. *Sci. Total Environ.* **2023**, *893*, 164853. [CrossRef]
130. Jones, T.R.; Poitras, J.; Paterson, D.; Southam, G. Historical Diamond Mine Waste Reveals Carbon Sequestration Resource in Kimberlite Residue. *Chem. Geol.* **2023**, *617*, 121270. [CrossRef]
131. Sundaram, S.; Thakur, I.S. Induction of Calcite Precipitation through Heightened Production of Extracellular Carbonic Anhydrase by CO_2 Sequestering Bacteria. *Bioresour. Technol.* **2018**, *253*, 368–371. [CrossRef] [PubMed]
132. Lam, L.; Ilies, M.A. Evaluation of the Impact of Esterases and Lipases from the Circulatory System against Substrates of Different Lipophilicity. *Int. J. Mol. Sci.* **2022**, *23*, 1262. [CrossRef] [PubMed]
133. Kaplan, A.; Reinhold, L. CO_2 Concentrating Mechanisms in Photosynthetic Microorganisms. *Annu. Rev. Plant Biol.* **1999**, *50*, 539–570. [CrossRef] [PubMed]
134. Supuran, C.T.; Capasso, C. An Overview of the Bacterial Carbonic Anhydrases. *Metabolites* **2017**, *7*, 56. [CrossRef]
135. Badger, M.R.; Hanson, D.; Price, G.D. Evolution and Diversity of CO_2 Concentrating Mechanisms in Cyanobacteria. *Funct. Plant Biol.* **2002**, *29*, 161–173. [CrossRef]
136. Klanchui, A.; Cheevadhanarak, S.; Prommeenate, P.; Meechai, A. Exploring Components of the CO_2-Concentrating Mechanism in Alkaliphilic Cyanobacteria Through Genome-Based Analysis. *Comput. Struct. Biotechnol. J.* **2017**, *15*, 340–350. [CrossRef]
137. Price, G.D.; Badger, M.R.; Woodger, F.J.; Long, B.M. Advances in Understanding the Cyanobacterial CO_2-Concentrating-Mechanism (CCM): Functional Components, Ci Transporters, Diversity, Genetic Regulation and Prospects for Engineering into Plants. *J. Exp. Bot.* **2008**, *59*, 1441–1461. [CrossRef]
138. Badger, M.R.; Price, G.D.; Long, B.M.; Woodger, F.J. The Environmental Plasticity and Ecological Genomics of the Cyanobacterial CO_2 Concentrating Mechanism. *J. Exp. Bot.* **2006**, *57*, 249–265. [CrossRef]
139. Capasso, C.; Supuran, C.T. An Overview of the Alpha-, Beta- and Gamma-Carbonic Anhydrases from Bacteria: Can Bacterial Carbonic Anhydrases Shed New Light on Evolution of Bacteria? *J. Enzym. Inhib. Med. Chem.* **2015**, *30*, 325–332. [CrossRef]
140. Sharma, A.; Bhattacharya, A.; Singh, S. Purification and Characterization of an Extracellular Carbonic Anhydrase from *Pseudomonas Fragi*. *Process Biochem.* **2009**, *44*, 1293–1297. [CrossRef]
141. Kupriyanova, E.; Villarejo, A.; Markelova, A.; Gerasimenko, L.; Zavarzin, G.; Samuelsson, G.; Los, D.A.; Pronina, N. Extracellular Carbonic Anhydrases of the Stromatolite-Forming Cyanobacterium Microcoleus Chthonoplastes. *Microbiology* **2007**, *153*, 1149–1156. [CrossRef] [PubMed]
142. Zhang, Z.; Lian, B.; Chen, M.; Li, X.; Li, Y. Bacillus Mucilaginosus Can Capture Atmospheric CO_2 by Carbonic Anhydrase. *Afr. J. Microbiol. Res.* **2011**, *5*, 106–112.
143. Li, W.; Yu, L.; He, Q.; Wu, Y.; Yuan, D.; Cao, J. Effects of Microbes and Their Carbonic Anhydrase on Ca^{2+} and Mg^{2+} Migration in Column-Built Leached Soil-Limestone Karst Systems. *Appl. Soil Ecol.* **2005**, *29*, 274–281. [CrossRef]

144. Nathan, V.K.; Ammini, P. Carbon Dioxide Sequestering Ability of Bacterial Carbonic Anhydrase in a Mangrove Soil Microcosm and Its Bio-Mineralization Properties. *Water Air Soil Pollut.* **2019**, *230*, 192. [CrossRef]
145. Zhu, J.; Sun, J.; Pang, C.; Li, Q.; Yang, Z.; Li, G. Isolation, Identification, and Carbonate Mineralization Characteristics of a Newly Carbonic Anhydrase-Producing Strain. *Appl. Biochem. Biotechnol.* **2024**, *196*, 8009–8025. [CrossRef]
146. Christianson, D.W.; Fierke, C.A. Carbonic Anhydrase: Evolution of the Zinc Binding Site by Nature and by Design. *Acc. Chem. Res.* **1996**, *29*, 331–339. [CrossRef]
147. Kiefer, L.L.; Paterno, S.A.; Fierke, C.A. Hydrogen Bond Network in the Metal Binding Site of Carbonic Anhydrase Enhances Zinc Affinity and Catalytic Efficiency. *J. Am. Chem. Soc.* **1995**, *117*, 6831–6837. [CrossRef]
148. Supuran, C.T.; Scozzafava, A.; Casini, A. Carbonic Anhydrase Inhibitors. *Med. Res. Rev.* **2003**, *23*, 146–189. [CrossRef]
149. Tupper, R.; Watts, R.W.E.; Wormall, A. Some Observations on the Zinc in Carbonic Anhydrase. *Biochem. J.* **1952**, *50*, 429–432. [CrossRef]
150. Håkansson, K.; Carlsson, M.; Svensson, L.A.; Liljas, A. Structure of Native and Apo Carbonic Anhydrase II and Structure of Some of Its Anion-Ligand Complexes. *J. Mol. Biol.* **1992**, *227*, 1192–1204. [CrossRef]
151. McCall, K.A.; Huang, C.; Fierke, C.A. Function and Mechanism of Zinc Metalloenzymes. *J. Nutr.* **2000**, *130*, 1437S–1446S. [CrossRef] [PubMed]
152. Dhami, N.; Reddy, M.; Mukherjee, A. Biomineralization of Calcium Carbonate Polymorphs by the Bacterial Strains Isolated from Calcareous Sites. *J. Microbiol. Biotechnol.* **2013**, *23*, 707–714. [CrossRef] [PubMed]
153. Zhao, J.; Lu, W.; Zhang, F.; Lu, C.; Du, J.; Zhu, R.; Sun, L. Evaluation of CO_2 Solubility-Trapping and Mineral-Trapping in Microbial-Mediated CO_2–Brine–Sandstone Interaction. *Mar. Pollut. Bull.* **2014**, *85*, 78–85. [CrossRef]
154. Achal, V.; Pan, X.; Lee, D.-J.; Kumari, D.; Zhang, D. Remediation of Cr(VI) from Chromium Slag by Biocementation. *Chemosphere* **2013**, *93*, 1352–1358. [CrossRef]
155. Park, I.-S.; Hausinger, R.P. Requirement of Carbon Dioxide for in Vitro Assembly of the Urease Nickel Metallocenter. *Science* **1995**, *267*, 1156–1158. [CrossRef]
156. Lal, R. Forest Soils and Carbon Sequestration. *For. Ecol. Manag.* **2005**, *220*, 242–258. [CrossRef]
157. Dhanwantri, K.; Sharma, P.; Mehta, S.; Prakash, P. Carbon Sequestration, Its Methods and Significance. In *Environmental Sustainability: Concepts, Principles, Evidences and Innovations*; Mishra, G.C., Ed.; Excellent Publishing House: New Delhi, India, 2014; pp. 94–98. ISBN 978-93-83083-75-6.
158. Jiao, N.; Robinson, C.; Azam, F.; Thomas, H.; Baltar, F.; Dang, H.; Hardman-Mountford, N.J.; Johnson, M.; Kirchman, D.L.; Koch, B.P.; et al. Mechanisms of Microbial Carbon Sequestration in the Ocean—Future Research Directions. *Biogeosciences* **2014**, *11*, 5285–5306. [CrossRef]
159. Ricour, F.; Guidi, L.; Gehlen, M.; DeVries, T.; Legendre, L. Century-Scale Carbon Sequestration Flux throughout the Ocean by the Biological Pump. *Nat. Geosci.* **2023**, *16*, 1105–1113. [CrossRef]
160. Jiao, N.; Azam, F. Microbial Carbon Pump and Its Significance for Carbon Sequestration in the Ocean. In *Microbial Carbon Pump in the Ocean*; Jiao, N., Azam, F., Sanders, S., Eds.; The American Association for the Advancement of Science: Washington, DC, USA, 2011.
161. Dhamu, V.; Qureshi, M.F.; Barckholtz, T.A.; Mhadeshwar, A.B.; Linga, P. Evaluating Liquid CO_2 Hydrate Formation Kinetics, Morphology, and Stability in Oceanic Sediments on a Lab Scale Using Top Injection. *Chem. Eng. J.* **2023**, *478*, 147200. [CrossRef]
162. Cunningham, A.B.; Gerlach, R.; Spangler, L.; Mitchell, A.C. Microbially Enhanced Geologic Containment of Sequestered Supercritical CO_2. *Energy Procedia* **2009**, *1*, 3245–3252. [CrossRef]
163. Benson, S.M.; Cole, D.R. CO_2 Sequestration in Deep Sedimentary Formations. *Elements* **2008**, *4*, 325–331. [CrossRef]
164. Pan, S.-Y.; Chang, E.E.; Chiang, P.-C. CO_2 Capture by Accelerated Carbonation of Alkaline Wastes: A Review on Its Principles and Applications. *Aerosol Air Qual. Res.* **2012**, *12*, 770–791. [CrossRef]
165. Bodor, M.; Santos, R.; Gerven, T.; Vlad, M. Recent Developments and Perspectives on the Treatment of Industrial Wastes by Mineral Carbonation—A Review. *Open Eng.* **2013**, *3*, 566–584. [CrossRef]
166. Gomes, H.I.; Mayes, W.M.; Rogerson, M.; Stewart, D.I.; Burke, I.T. Alkaline Residues and the Environment: A Review of Impacts, Management Practices and Opportunities. *J. Clean. Prod.* **2016**, *112*, 3571–3582. [CrossRef]
167. Eloneva, S.; Puheloinen, E.-M.; Kanweva, J.; Ekroos, A.; Zevenhoven, R.; Fogelholm, C.-J. Co-Utilisation of CO_2 and Steelmaking Slags for Production of Pure $CaCO_3$—Legislative Issues. *J. Clean. Prod.* **2010**, *18*, 1833–1839. [CrossRef]
168. Rashid, M.I.; Yaqoob, Z.; Mujtaba, M.A.; Fayaz, H.; Saleel, C.A. Developments in Mineral Carbonation for Carbon Sequestration. *Heliyon* **2023**, *9*, e21796. [CrossRef]
169. Chang, R.; Kim, S.; Lee, S.; Choi, S.; Kim, M.; Park, Y. Calcium Carbonate Precipitation for CO_2 Storage and Utilization: A Review of the Carbonate Crystallization and Polymorphism. *Front. Energy Res.* **2017**, *5*, 17. [CrossRef]
170. Mayes, W.M.; Younger, P.L. Buffering of Alkaline Steel Slag Leachate across a Natural Wetland. *Environ. Sci. Technol.* **2006**, *40*, 1237–1243. [CrossRef]

171. Lim, M.; Han, G.-C.; Ahn, J.-W.; You, K.-S. Environmental Remediation and Conversion of Carbon Dioxide (CO_2) into Useful Green Products by Accelerated Carbonation Technology. *Int. J. Environ. Res. Public Health* **2010**, *7*, 203–228. [CrossRef]
172. Bobicki, E.R.; Liu, Q.; Xu, Z.; Zeng, H. Carbon Capture and Storage Using Alkaline Industrial Wastes. *Prog. Energy Combust. Sci.* **2012**, *38*, 302–320. [CrossRef]
173. Eloneva, S.; Teir, S.; Salminen, J.; Fogelholm, C.-J.; Zevenhoven, R. Fixation of CO_2 by Carbonating Calcium Derived from Blast Furnace Slag. *Energy* **2008**, *33*, 1461–1467. [CrossRef]
174. Olajire, A.A. A Review of Mineral Carbonation Technology in Sequestration of CO_2. *J. Pet. Sci. Eng.* **2013**, *109*, 364–392. [CrossRef]
175. Sanna, A.; Uibu, M.; Caramanna, G.; Kuusik, R.; Maroto-Valer, M.M. A Review of Mineral Carbonation Technologies to Sequester CO_2. *Chem. Soc. Rev.* **2014**, *43*, 8049–8080. [CrossRef] [PubMed]
176. Khudhur, F.W.K.; MacDonald, J.M.; Macente, A.; Daly, L. The Utilization of Alkaline Wastes in Passive Carbon Capture and Sequestration: Promises, Challenges and Environmental Aspects. *Sci. Total Environ.* **2022**, *823*, 153553. [CrossRef]
177. Wilson, S.A.; Dipple, G.M.; Power, I.M.; Thom, J.M.; Anderson, R.G.; Raudsepp, M.; Gabites, J.E.; Southam, G. Carbon Dioxide Fixation within Mine Wastes of Ultramafic-Hosted Ore Deposits: Examples from the Clinton Creek and Cassiar Chrysotile Deposits, Canada. *Econ. Geol.* **2009**, *104*, 95–112. [CrossRef]
178. Power, I.M.; Harrison, A.L.; Dipple, G.M. Accelerating Mineral Carbonation Using Carbonic Anhydrase. *Environ. Sci. Technol.* **2016**, *50*, 2610–2618. [CrossRef]
179. Li, X.; Bertos, M.F.; Hills, C.D.; Carey, P.J.; Simon, S. Accelerated Carbonation of Municipal Solid Waste Incineration Fly Ashes. *Waste Manag.* **2007**, *27*, 1200–1206. [CrossRef]
180. Rendek, E.; Ducom, G.; Germain, P. Carbon Dioxide Sequestration in Municipal Solid Waste Incinerator (MSWI) Bottom Ash. *J. Hazard. Mater.* **2006**, *128*, 73–79. [CrossRef]
181. Liu, W.; Su, S.; Xu, K.; Chen, Q.; Xu, J.; Sun, Z.; Wang, Y.; Hu, S.; Wang, X.; Xue, Y.; et al. CO_2 Sequestration by Direct Gas–Solid Carbonation of Fly Ash with Steam Addition. *J. Clean. Prod.* **2018**, *178*, 98–107. [CrossRef]
182. Veetil, S.P.; Pasquier, L.-C.; Blais, J.-F.; Cecchi, E.; Kentish, S.; Mercier, G. Direct Gas–Solid Carbonation of Serpentinite Residues in the Absence and Presence of Water Vapor: A Feasibility Study for Carbon Dioxide Sequestration. *Environ. Sci. Pollut. Res.* **2015**, *22*, 13486–13495. [CrossRef]
183. Fernández Bertos, M.; Li, X.; Simons, S.J.R.; Hills, C.D.; Carey, P.J. Investigation of Accelerated Carbonation for the Stabilisation of MSW Incinerator Ashes and the Sequestration of CO_2. *Green Chem.* **2004**, *6*, 428–436. [CrossRef]
184. Azdarpour, A.; Asadullah, M.; Mohammadian, E.; Hamidi, H.; Junin, R.; Karaei, M.A. A Review on Carbon Dioxide Mineral Carbonation through pH-Swing Process. *Chem. Eng. J.* **2015**, *279*, 615–630. [CrossRef]
185. Fagerlund, J.; Nduagu, E.; Romão, I.; Zevenhoven, R. A Stepwise Process for Carbon Dioxide Sequestration Using Magnesium Silicates. *Front. Chem. Eng. China* **2010**, *4*, 133–141. [CrossRef]
186. Ben Ghacham, A.; Cecchi, E.; Pasquier, L.-C.; Blais, J.-F.; Mercier, G. CO_2 Sequestration Using Waste Concrete and Anorthosite Tailings by Direct Mineral Carbonation in Gas–Solid–Liquid and Gas–Solid Routes. *J. Environ. Manag.* **2015**, *163*, 70–77. [CrossRef]
187. El-Naas, M.H.; El Gamal, M.; Hameedi, S.; Mohamed, A.-M.O. CO_2 Sequestration Using Accelerated Gas-Solid Carbonation of Pre-Treated EAF Steel-Making Bag House Dust. *J. Environ. Manag.* **2015**, *156*, 218–224. [CrossRef]
188. Baciocchi, R.; Polettini, A.; Pomi, R.; Prigiobbe, V.; Von Zedwitz, V.N.; Steinfeld, A. CO_2 Sequestration by Direct Gas−Solid Carbonation of Air Pollution Control (APC) Residues. *Energy Fuels* **2006**, *20*, 1933–1940. [CrossRef]
189. Ho, H.-J.; Iizuka, A.; Shibata, E.; Tomita, H.; Takano, K.; Endo, T. CO_2 Utilization via Direct Aqueous Carbonation of Synthesized Concrete Fines under Atmospheric Pressure. *ACS Omega* **2020**, *5*, 15877–15890. [CrossRef]
190. Li, J.; Jacobs, A.D.; Hitch, M. Direct Aqueous Carbonation on Olivine at a CO_2 Partial Pressure of 6.5 MPa. *Energy* **2019**, *173*, 902–910. [CrossRef]
191. Song, K.; Jang, Y.-N.; Kim, W.; Lee, M.G.; Shin, D.; Bang, J.-H.; Jeon, C.W.; Chae, S.C. Factors Affecting the Precipitation of Pure Calcium Carbonate during the Direct Aqueous Carbonation of Flue Gas Desulfurization Gypsum. *Energy* **2014**, *65*, 527–532. [CrossRef]
192. Huijgen, W.J.J.; Witkamp, G.-J.; Comans, R.N.J. Mineral CO_2 Sequestration by Steel Slag Carbonation. *Environ. Sci. Technol.* **2005**, *39*, 9676–9682. [CrossRef]
193. Yadav, V.S.; Prasad, M.; Khan, J.; Amritphale, S.S.; Singh, M.; Raju, C.B. Sequestration of Carbon Dioxide (CO_2) Using Red Mud. *J. Hazard. Mater.* **2010**, *176*, 1044–1050. [CrossRef] [PubMed]
194. Uibu, M.; Velts, O.; Kuusik, R. Developments in CO_2 Mineral Carbonation of Oil Shale Ash. *J. Hazard. Mater.* **2010**, *174*, 209–214. [CrossRef] [PubMed]
195. Montes-Hernandez, G.; Pérez-López, R.; Renard, F.; Nieto, J.M.; Charlet, L. Mineral Sequestration of CO_2 by Aqueous Carbonation of Coal Combustion Fly-Ash. *J. Hazard. Mater.* **2009**, *161*, 1347–1354. [CrossRef]
196. Li, Z.; Chen, J.; Lv, Z.; Tong, Y.; Ran, J.; Qin, C. Evaluation on Direct Aqueous Carbonation of Industrial/Mining Solid Wastes for CO_2 Mineralization. *J. Ind. Eng. Chem.* **2023**, *122*, 359–365. [CrossRef]

197. Ho, H.-J.; Iizuka, A.; Shibata, E.; Tomita, H.; Takano, K.; Endo, T. Utilization of CO_2 in Direct Aqueous Carbonation of Concrete Fines Generated from Aggregate Recycling: Influences of the Solid–Liquid Ratio and CO_2 Concentration. *J. Clean. Prod.* **2021**, *312*, 127832. [CrossRef]
198. Ho, H.-J.; Iizuka, A.; Shibata, E. Utilization of Low-Calcium Fly Ash via Direct Aqueous Carbonation with a Low-Energy Input: Determination of Carbonation Reaction and Evaluation of the Potential for CO_2 Sequestration and Utilization. *J. Environ. Manag.* **2021**, *288*, 112411. [CrossRef]
199. O'Connor, W.K.; Dahlin, D.C.; Nilsen, D.N.; Rush, G.E.; Walters, R.P.; Turner, P.C. *CO_2 Storage in Solid Form: A Study of Direct Mineral Carbonation*; CSIRO: Collinwood, Australia, 2000.
200. Mun, M.; Cho, H.; Kwon, J. Study on Characteristics of Various Extractants for Mineral Carbonation of Industrial Wastes. *J. Environ. Chem. Eng.* **2017**, *5*, 3803–3821. [CrossRef]
201. Park, A.-H.A.; Fan, L.-S. CO_2 Mineral Sequestration: Physically Activated Dissolution of Serpentine and pH Swing Process. *Chem. Eng. Sci.* **2004**, *59*, 5241–5247. [CrossRef]
202. Wang, X.; Maroto-Valer, M.M. Dissolution of Serpentine Using Recyclable Ammonium Salts for CO_2 Mineral Carbonation. *Fuel* **2011**, *90*, 1229–1237. [CrossRef]
203. Bosecker, K. Bioleaching: Metal Solubilization by Microorganisms. *FEMS Microbiol. Rev.* **1997**, *20*, 591–604. [CrossRef]
204. Schwartzman, D.W.; Volk, T. Biotic Enhancement of Weathering and the Habitability of Earth. *Nature* **1989**, *340*, 457–460. [CrossRef]
205. Chiang, Y.W.; Santos, R.M.; Monballiu, A.; Ghyselbrecht, K.; Martens, J.A.; Mattos, M.L.T.; Gerven, T.V.; Meesschaert, B. Effects of Bioleaching on the Chemical, Mineralogical and Morphological Properties of Natural and Waste-Derived Alkaline Materials. *Miner. Eng.* **2013**, *48*, 116–125. [CrossRef]
206. Power, I.M.; McCutcheon, J.; Harrison, A.L.; Wilson, S.; Dipple, G.M.; Kelly, S.; Southam, C.; Southam, G. Strategizing Carbon-Neutral Mines: A Case for Pilot Projects. *Minerals* **2014**, *4*, 399–436. [CrossRef]
207. Power, I.M.; Dipple, G.M.; Southam, G. Bioleaching of Ultramafic Tailings by Acidithiobacillus Spp. for CO_2 Sequestration. *Environ. Sci. Technol.* **2010**, *44*, 456–462. [CrossRef]
208. Fang, C.; Achal, V. Enhancing Carbon Neutrality: A Perspective on the Role of Microbially Induced Carbonate Precipitation (MICP). *Biogeotechnics* **2024**, *2*, 100083. [CrossRef]
209. Achal, V.; Pan, X.; Fu, Q.; Zhang, D. Biomineralization Based Remediation of As(III) Contaminated Soil by Sporosarcina Ginsengisoli. *J. Hazard. Mater.* **2012**, *201–202*, 178–184. [CrossRef]
210. Achal, V.; Pan, X.; Zhang, D. Bioremediation of Strontium (Sr) Contaminated Aquifer Quartz Sand Based on Carbonate Precipitation Induced by Sr Resistant *Halomonas* sp. *Chemosphere* **2012**, *89*, 764–768. [CrossRef]
211. Stabnikov, V.; Jian, C.; Ivanov, V.; Li, Y. Halotolerant, Alkaliphilic Urease-Producing Bacteria from Different Climate Zones and Their Application for Biocementation of Sand. *World J. Microbiol. Biotechnol.* **2013**, *29*, 1453–1460. [CrossRef]
212. Duan, Y.; Niu, L.; Li, B.; He, Y.; Xu, X.; Yu, C.; Wang, Z.; Xiao, C.; Zheng, C. Montmorillonite-Coupled Microbially Induced Carbonate Precipitation (MICP) Enhanced Contaminant Removal and Carbon Capture in Cyanide Tailings. *J. Environ. Chem. Eng.* **2024**, *12*, 113498. [CrossRef]
213. Achal, V.; Mukherjee, A. A Review of Microbial Precipitation for Sustainable Construction. *Constr. Build. Mater.* **2015**, *93*, 1224–1235. [CrossRef]
214. Kang, B.; Zha, F.; Deng, W.; Wang, R.; Sun, X.; Lu, Z. Biocementation of Pyrite Tailings Using Microbially Induced Calcite Carbonate Precipitation. *Molecules* **2022**, *27*, 3608. [CrossRef] [PubMed]
215. Maureira, A.; Zapata, M.; Olave, J.; Jeison, D.; Wong, L.-S.; Panico, A.; Hernández, P.; Cisternas, L.A.; Rivas, M. MICP Mediated by Indigenous Bacteria Isolated from Tailings for Biocementation for Reduction of Wind Erosion. *Front. Bioeng. Biotechnol.* **2024**, *12*, 1393334. [CrossRef] [PubMed]
216. Mwandira, W.; Nakashima, K.; Kawasaki, S.; Ito, M.; Sato, T.; Igarashi, T.; Banda, K.; Chirwa, M.; Nyambe, I.; Nakayama, S.; et al. Efficacy of Biocementation of Lead Mine Waste from the Kabwe Mine Site Evaluated Using *Pararhodobacter* sp. *Environ. Sci. Pollut. Res. Int.* **2019**, *26*, 15653–15664. [CrossRef] [PubMed]
217. De Muynck, W.; De Belie, N.; Verstraete, W. Microbial Carbonate Precipitation in Construction Materials: A Review. *Ecol. Eng.* **2010**, *36*, 118–136. [CrossRef]
218. Bandyopadhyay, A.; Saha, A.; Ghosh, D.; Dam, B.; Samanta, A.K.; Dutta, S. Microbial Repairing of Concrete & Its Role in CO_2 Sequestration: A Critical Review. *Beni-Suef Univ. J. Basic Appl. Sci.* **2023**, *12*, 7. [CrossRef]
219. Hussain, A.; Ali, D.; Koner, S.; Hseu, Z.-Y.; Hsu, B.-M. Microbial Induce Carbonate Precipitation Derive Bio-Concrete Formation: A Sustainable Solution for Carbon Sequestration and Eco-Friendly Construction. *Environ. Res* **2025**, *270*, 121006. [CrossRef]
220. Wong, P.Y.; Mal, J.; Sandak, A.; Luo, L.; Jian, J.; Pradhan, N. Advances in Microbial Self-Healing Concrete: A Critical Review of Mechanisms, Developments, and Future Directions. *Sci. Total Environ.* **2024**, *947*, 174553. [CrossRef]
221. Fu, T.; Saracho, A.C.; Haigh, S.K. Microbially Induced Carbonate Precipitation (MICP) for Soil Strengthening: A Comprehensive Review. *Biogeotechnics* **2023**, *1*, 100002. [CrossRef]

222. Cheng, L.; Shahin, M.A.; Mujah, D. Influence of Key Environmental Conditions on Microbially Induced Cementation for Soil Stabilization. *J. Geotech. Geoenviron. Eng.* **2017**, *143*, 04016083. [CrossRef]
223. DeJong, J.T.; Mortensen, B.M.; Martinez, B.C.; Nelson, D.C. Bio-Mediated Soil Improvement. *Ecol. Eng.* **2010**, *36*, 197–210. [CrossRef]
224. Ramanan, R.; Kannan, K.; Sivanesan, S.D.; Mudliar, S.; Kaur, S.; Tripathi, A.K.; Chakrabarti, T. Bio-Sequestration of Carbon Dioxide Using Carbonic Anhydrase Enzyme Purified from Citrobacter Freundii. *World J. Microbiol. Biotechnol.* **2009**, *25*, 981–987. [CrossRef]
225. Gilmour, K.A.; Ghimire, P.S.; Wright, J.; Haystead, J.; Dade-Robertson, M.; Zhang, M.; James, P. Microbially Induced Calcium Carbonate Precipitation through CO_2 Sequestration via an Engineered Bacillus Subtilis. *Microb. Cell Factories* **2024**, *23*, 168. [CrossRef] [PubMed]
226. Li, W.; Chen, W.-S.; Zhou, P.-P.; Yu, L.-J. Influence of Enzyme Concentration on Bio-Sequestration of CO_2 in Carbonate Form Using Bacterial Carbonic Anhydrase. *Chem. Eng. J.* **2013**, *232*, 149–156. [CrossRef]
227. Silva-Castro, G.A.; Uad, I.; Gonzalez-Martinez, A.; Rivadeneyra, A.; Gonzalez-Lopez, J.; Rivadeneyra, M.A. Bioprecipitation of Calcium Carbonate Crystals by Bacteria Isolated from Saline Environments Grown in Culture Media Amended with Seawater and Real Brine. *BioMed Res. Int.* **2015**, *2015*, 816102. [CrossRef]
228. Zheng, T.; Qian, C. Influencing Factors and Formation Mechanism of $CaCO_3$ Precipitation Induced by Microbial Carbonic Anhydrase. *Process Biochem.* **2020**, *91*, 271–281. [CrossRef]
229. Xiao, L.; Lian, B. Heterologously Expressed Carbonic Anhydrase from *Bacillus mucilaginosus* Promoting $CaCO_3$ Formation by Capturing Atmospheric CO_2. *Carbonates Evaporites* **2016**, *31*, 39–45. [CrossRef]
230. Abdelsamad, R.; Disi, Z.A.; Abu-Dieyeh, M.; Al-Ghouti, M.A.; Zouari, N. Evidencing the Role of Carbonic Anhydrase in the Formation of Carbonate Minerals by Bacterial Strains Isolated from Extreme Environments in Qatar. *Heliyon* **2022**, *8*, e11151. [CrossRef]
231. Huang, L.; Li, F.; Ji, C.; Wang, Y.; Yang, G. Carbon Isotope Fractionation and Its Tracer Significance to Carbon Source during Precipitation of Calcium Carbonate in the Presence of *Bacillus Cereus* LV-1. *Chem. Geol.* **2022**, *609*, 121029. [CrossRef]
232. Yang, G.; Li, L.; Li, F.; Zhang, C.; Lyu, J. Mechanism of Carbonate Mineralization Induced by Microbes: Taking Curvibacter Lanceolatus Strain HJ-1 as an Example. *Micron* **2021**, *140*, 102980. [CrossRef]
233. Mitchell, A.C.; Dideriksen, K.; Spangler, L.H.; Cunningham, A.B.; Gerlach, R. Microbially Enhanced Carbon Capture and Storage by Mineral-Trapping and Solubility-Trapping. *Environ. Sci. Technol.* **2010**, *44*, 5270–5276. [CrossRef]
234. Zhang, Y.; Hu, X.; Wang, Y.; Jiang, N. A Critical Review of Biomineralization in Environmental Geotechnics: Applications, Trends, and Perspectives. *Biogeotechnics* **2023**, *1*, 100003. [CrossRef]
235. Government of Canada; Innovation, Science and Economic Development Canada; Cement Association of Canada. *Roadmap to Net-Zero Carbon Concrete by 2050*; Innovation, Science and Economic Development Canada: Ottawa, ON, Canada, 2024.
236. del Strother, P. 2—Manufacture of Portland Cement. In *Lea's Chemistry of Cement and Concrete*, 15th ed.; Hewlett, P.C., Liska, M., Eds.; Butterworth-Heinemann: Oxford, UK, 2019; pp. 31–56. ISBN 978-0-08-100773-0.
237. Hendriks, C.A.; Worrell, E.; Price, L.; Martin, N.; Ozawa Meida, L.; De Jager, D.; Riemer, P. Emission Reduction of Greenhouse Gases from the Cement Industry. In *Greenhouse Gas Control Technologies 4*; Elsevier: Amsterdam, The Netherlands, 1999; pp. 939–944. ISBN 978-0-08-043018-8.
238. Sharma, M.; Satyam, N.; Reddy, K.R. State of the Art Review of Emerging and Biogeotechnical Methods for Liquefaction Mitigation in Sands. *J. Hazard. Toxic Radioact. Waste* **2021**, *25*, 03120002. [CrossRef]
239. Burbank, M.B.; Weaver, T.J.; Green, T.L.; Williams, B.C.; Crawford, R.L. Precipitation of Calcite by Indigenous Microorganisms to Strengthen Liquefiable Soils. *Geomicrobiol. J.* **2011**, *28*, 301–312. [CrossRef]
240. Zhang, K.; Tang, C.-S.; Jiang, N.-J.; Pan, X.-H.; Liu, B.; Wang, Y.-J.; Shi, B. Microbial-induced Carbonate Precipitation (MICP) Technology: A Review on the Fundamentals and Engineering Applications. *Environ. Earth Sci.* **2023**, *82*, 229. [CrossRef]
241. Liu, J.; Zhen, B.; Qiu, H.; Zhou, X.; Zhang, H. Impact of Waterlogging and Heat Stress on Rice Rhizosphere Microbiome Assembly and Potential Function in Carbon and Nitrogen Transformation. *Arch. Agron. Soil Sci.* **2023**, *69*, 1920–1932. [CrossRef]
242. Liu, B.; Tang, C.-S.; Pan, X.-H.; Zhu, C.; Cheng, Y.-J.; Xu, J.-J.; Shi, B. Potential Drought Mitigation through Microbial Induced Calcite Precipitation—MICP. *Water Resour. Res.* **2021**, *57*, e2020WR029434. [CrossRef]